Available online at www.sciencedirect.com
ScienceDirect
Comput. Methods Appl. Mech. Engrg. 372 (2020) 113407
Computer methods in applied mechanics and engineering
www.elsevier.com/locate/cma

A coupled multipoint stress–multipoint flux mixed finite element method for the Biot system of poroelasticity

Ilona Ambartsumyan[a,b,1], Eldar Khattatov[a,b,1], Ivan Yotov[a,*,1]

[a] *Department of Mathematics, University of Pittsburgh, Pittsburgh, PA 15260, USA*
[b] *Oden Institute for Computational Engineering and Sciences, The University of Texas at Austin, Austin, TX 78712, USA*

Available online xxxx

Abstract

We present a mixed finite element method for a five-field formulation of the Biot system of poroelasticity that reduces to a cell-centered pressure–displacement system on simplicial and quadrilateral grids. A mixed stress–displacement–rotation formulation for elasticity with weak stress symmetry is coupled with a mixed velocity–pressure Darcy formulation. The spatial discretization is based on combining the multipoint stress mixed finite element (MSMFE) method for elasticity and the multipoint flux mixed finite element (MFMFE) method for Darcy flow. It uses the lowest order Brezzi–Douglas–Marini mixed finite element spaces for the poroelastic stress and Darcy velocity, piecewise constant displacement and pressure, and continuous piecewise linear or bilinear rotation. A vertex quadrature rule is applied to the velocity, stress, and stress–rotation bilinear forms, which block-diagonalizes the corresponding matrices and allows for local velocity, stress, and rotation elimination. This leads to a cell-centered positive-definite system for pressure and displacement at each time step. We perform error analysis for the semidiscrete and fully discrete formulations, establishing first order convergence for all variables in their natural norms. The numerical tests confirm the theoretical convergence rates and illustrate the locking-free property of the method.
© 2020 Elsevier B.V. All rights reserved.

Keywords: Mixed finite elements; Cell-centered finite differences; Multipoint stress; Multipoint flux; Poroelasticity

1. Introduction

The Biot system of poroelasticity [8,46] models fluid flow within deformable porous media. It has been extensively studied in the literature due to its wide range of applications. Examples include geosciences, such as groundwater cleanup, hydraulic fracturing, and carbon sequestration, as well as biomedical applications, such as modeling of arterial flows and organ tissue. The system consists of an equilibrium equation for the solid and a mass balance equation for the fluid. This is a fully coupled system, as the fluid pressure contributes to the solid stress, while the divergence of the solid displacement affects the fluid content. There is a large literature on the numerical solution of the Biot system. Schemes for the two-field displacement–pressure formulation include finite difference [18], finite volume [36], and finite element methods [31,44]. The finite element methods are

* Corresponding author.
E-mail addresses: ila6@pitt.edu, ailona@austin.utexas.edu (I. Ambartsumyan), elk58@pitt.edu, ekhattatov@austin.utexas.edu (E. Khattatov), yotov@math.pitt.edu (I. Yotov).
[1] Partially supported by DOE, USA grant DE-FG02-04ER25618 and NSF, USA grant DMS 1818775.

https://doi.org/10.1016/j.cma.2020.113407
0045-7825/© 2020 Elsevier B.V. All rights reserved.

either based on inf–sup stable pairs [31,44] or employ a suitable stabilization to avoid pressure oscillations [44]. The three-field displacement–pressure–Darcy velocity formulation has also been studied extensively. It has the advantage that stable mixed finite element spaces for the Darcy velocity and the pressure can be utilized, resulting in accurate fluid velocity and local mass conservation. Various choices of displacement discretizations have been used in the three-field formulation, including continuous, [38,39,45,55], nonconforming [20,27,53], and discontinuous elements [29,40]. The last two choices provide locking-free approximations. Alternatively, stabilized continuous displacement elements can be used to suppress pressure oscillations [45,55]. Locking-free discretizations for a different three-field displacement–pressure–total pressure formulation are developed in [28,37]. A least squares method based on a stress–displacement–velocity–pressure formulation is developed in [24]. More recently, fully-mixed formulations of the Biot system have been studied [25,54]. In [54], a stress–displacement mixed elasticity formulation is coupled with a velocity–pressure mixed Darcy model. This approach is extended in [25], where a weakly symmetric stress–displacement–rotation elasticity formulation is considered.

In this paper we develop a new fully-mixed finite element method for the quasistatic Biot system of poroelasticity. The advantages of fully-mixed approximations include locking-free behavior, robustness with respect to the physical parameters, local mass and momentum conservation, and accurate stress and velocity approximations with continuous normal components across element edges or faces. They can also handle discontinuous full tensor permeabilities and Lamé coefficients that are often encountered in modeling subsurface flows. A disadvantage of fully-mixed methods is that they result in large algebraic systems of saddle point type at each time step. In particular, the methods developed in [54] and [25] involve four-field and five-field formulations, respectively. Our goal is to develop a fully-mixed method that can be reduced to a positive definite cell-centered displacement–pressure system. As a result, the method inherits all the advantages of fully-mixed finite element methods, while having a significantly reduced computational cost. In fact, the number of unknowns in the reduced algebraic system is smaller than in any of the aforementioned finite element methods. It is comparable to the cost of the finite volume method developed in [36].

Our approach is based on the five-field formulation proposed in [25]. We couple the recently developed multipoint stress mixed finite element (MSMFE) method for elasticity [2,3] with weak stress symmetry and the multipoint flux mixed finite element (MFMFE) method for Darcy flow [21,50,52]. The MFMFE method is related to the finite volume multipoint flux approximation (MPFA) method [1,15]. The MFMFE method provides a variational formulation for the MPFA method, which allows for utilizing mixed finite element tools for its analysis. It uses the lowest order Brezzi–Douglas–Marini $\mathcal{BDM}_1$ [12,33] spaces for the Darcy velocity and piecewise constant pressure. The vertex quadrature rule for the velocity bilinear form gives a block-diagonal mass matrix with blocks associated with the mesh vertices and allows for local velocity elimination, resulting in a cell-centered pressure system. The MFMFE method is analyzed on simplices and smooth quadrilateral and hexahedral grids, i.e., with elements that are $O(h^2)$-perturbations of parallelograms, in [21,52]. A similar approach on simplices is proposed in [13]. A non-symmetric version of the MFMFE method for general quadrilateral and hexahedral grids is developed in [50]; see also an alternative formulation based on a broken Raviart–Thomas velocity space in [23]. The MSMFE method for elasticity with weak stress symmetry was recently developed in [3] on simplices and in [2] on smooth quadrilateral grids. It uses $\mathcal{BDM}_1$ elements for the stress, piecewise constant displacement, and continuous piecewise linear rotation. The vertex quadrature rule is applied for the stress bilinear form, as well as the two stress–rotation bilinear forms. This allows for local stress and rotation elimination around the mesh vertices, resulting in a cell-centered displacement system. The development of the MSMFE method was motivated by the finite volume multipoint stress approximation (MPSA) method for elasticity introduced in [34] and analyzed in [35] as a discontinuous Galerkin (DG) method. A weak symmetry MPSA method, which is more closely related to the MSMFE method has been developed in [22].

In this work we develop and analyze a coupled MSMFE–MFMFE method for the Biot system of poroelasticity. Starting with the five-field stress–displacement–rotation–velocity–pressure formulation from [25], we employ the vertex quadrature rule for the stress, stress–rotation, and velocity bilinear forms. Since the stress, rotation, and velocity degrees of freedom can be associated with the mesh vertices, the quadrature rule localizes their interaction around the vertices, resulting in block-diagonal matrices. The stress and velocity, and consequently the rotation, can then be locally eliminated by solving small vertex-based linear systems. This procedure reduces the five-field saddle point system to a cell-centered displacement–pressure system. The elimination procedure resembles the approach in the finite volume method for the Biot system developed in [36], which couples the MPSA and MPFA methods,

although the method there is not based on weak symmetry and does not explicitly involve rotations. We also note that in our method we utilize a symmetric quadrature rule, as in the symmetric MFMFE method [21,52] and the MSMFE method [2,3]. As the individual methods, our coupled method is suitable for simplicial grids in two and three dimensions and quadrilateral grids with elements that are $O(h^2)$-perturbations of parallelograms. While a non-symmetric MFMFE method on general quadrilaterals and hexahedra is available [50], such non-symmetric MSMFE method for elasticity has not yet been developed.

We perform solvability, stability, and error analysis for the semidiscrete continuous-in-time and the fully discrete methods. The well-posedness of the semidiscrete formulation utilizes techniques from degenerate evolution operators [47,48]. For this purpose, we differentiate in time the constitutive elasticity equation and introduce as new variables the time derivatives of the displacement and the rotation. Stability is obtained for all variables in their natural spatial norms in both $L^2(0,T)$ and $L^\infty(0,T)$. In order to obtain control of the divergence of the Darcy velocity, a bound on the time derivative of the pressure is first derived, using time differentiation of the rest of the equations. First order spatial convergence is proven for all variables by combining stability arguments with bounds on the quadrature and approximation errors. It is important to note that the stability and convergence bounds are independent of the storativity coefficient c_0 and are valid even for $c_0 = 0$. As the regime of small c_0 results in locking effects [41], our theory confirms the locking-free property of the method. We also present the fully-discrete scheme, based on backward Euler time discretization. The analysis of the fully-discrete scheme uses the framework developed for the semidiscrete formulation, combined with standard tools for treating the discrete time derivatives.

The rest of the paper is organized as follows. The Biot system and its fully mixed five-field weak formulation are presented in Section 2. The semidiscrete MSMFE–MFMFE method is developed in Section 3. Its solvability and stability are established in Sections 4 and 5, respectively. The error analysis for the semidiscrete method is carried out in Section 6. Section 7 is devoted to the fully-discrete MSMFE–MFMFE method, where in addition to its analysis, the procedure for reducing the algebraic system to a cell-centered displacement–pressure system is presented. It is further shown that the resulting system is positive definite. Numerical results that confirm the theoretical convergence rates and illustrate the robustness with respect to c_0 and the locking-free behavior of the method are presented in Section 8.

2. Model problem and a fully mixed weak formulation

In this section we describe the poroelasticity system and its fully mixed formulation based on a weak stress symmetry, Let Ω be a simply connected bounded domain of $\mathbb{R}^d$, $d = 2, 3$, occupied by a poroelastic media saturated with fluid. Let $\mathbb{M}$, $\mathbb{S}$, and $\mathbb{N}$ be the spaces of real $d \times d$ matrices, symmetric matrices, and skew-symmetric matrices, respectively. The divergence operator $\operatorname{div} : \mathbb{R}^d \to \mathbb{R}$ is the usual divergence for vector fields. It also acts on matrix fields, $\operatorname{div} : \mathbb{M} \to \mathbb{R}^d$ by applying the divergence row-wise. We will also utilize the operator curl acting on scalar fields in two dimensions, $\operatorname{curl} : \mathbb{R} \to \mathbb{R}^2$, defined as $\operatorname{curl}\phi = (\partial_2\phi, -\partial_1\phi)$.

The stress–strain constitutive relationship for the poroelastic body is

$$A\sigma_e = \epsilon(u), \tag{2.1}$$

where at each point $x \in \Omega$, $A(x) : \mathbb{S} \to \mathbb{S}$, extendible to $A(x) : \mathbb{M} \to \mathbb{M}$, is a symmetric, bounded and uniformly positive definite linear operator representing the compliance tensor, σ_e is the elastic stress, u is the solid displacement, and $\epsilon(u) = \frac{1}{2}(\nabla u + \nabla u^T)$. In the case of a homogeneous and isotropic body,

$$A\sigma = \frac{1}{2\mu}\left(\sigma - \frac{\lambda}{2\mu + d\lambda}\operatorname{tr}(\sigma) I\right),$$

where I is the $d \times d$ identity matrix and $\mu > 0, \lambda \geq 0$ are the Lamé coefficients. In this case the elastic stress is $\sigma_e = 2\mu\epsilon(u) + \lambda \operatorname{div} u\, I$. The poroelastic stress, which includes the effect of the fluid pressure p, is given as

$$\sigma = \sigma_e - \alpha p I, \tag{2.2}$$

where $0 < \alpha \leq 1$ is the Biot–Willis constant.

Given a vector field f representing the body forces and a source term q, the quasi-static Biot system [8] that governs the fluid flow within the poroelastic media is as follows:

$$-\operatorname{div}\sigma = f \quad \text{in } \Omega \times (0,T], \tag{2.3}$$

$$K^{-1}z + \nabla p = 0 \quad \text{in } \Omega \times (0,T], \tag{2.4}$$

$$\frac{\partial}{\partial t}(c_0 p + \alpha \operatorname{div} u) + \operatorname{div} z = q \quad \text{in } \Omega \times (0,T], \tag{2.5}$$

where z is the Darcy velocity, $c_0 \geq 0$ is a mass storativity coefficient, and K is a symmetric and positive definite tensor representing the permeability of the porous media divided by the fluid viscosity. The system is closed with the boundary conditions

$$u = g_u \quad \text{on } \Gamma_D^{displ} \times (0,T], \qquad \sigma n = 0 \quad \text{on } \Gamma_N^{stress} \times (0,T], \tag{2.6}$$

$$p = g_p \quad \text{on } \Gamma_D^{pres} \times (0,T], \qquad z \cdot n = 0 \quad \text{on } \Gamma_N^{vel} \times (0,T], \tag{2.7}$$

and the initial condition $p(x,0) = p_0(x)$ in Ω, where $\Gamma_D^{displ} \cup \Gamma_N^{stress} = \Gamma_D^{pres} \cup \Gamma_N^{vel} = \partial\Omega$ and n is the outward unit normal vector field on $\partial\Omega$. To avoid technical issues due to non-uniqueness in the case of pure Neumann boundary conditions, we assume that $|\Gamma_D^*| > 0$, for $* = \{displ, pres\}$. We note that Eqs. (2.3) and (2.4), which do not include time derivatives, are assumed to hold at $t = 0$. This is used to construct compatible initial data for the rest of the variables. The well posedness of the above system has been studied in [46].

Throughout the paper, C denotes a generic positive constant that is independent of the discretization parameter h. We will also use the following standard notation. For a domain $G \subset \mathbb{R}^d$, the $L^2(G)$ inner product and norm for scalar, vector, or tensor valued functions are denoted $(\cdot,\cdot)_G$ and $\|\cdot\|_G$, respectively. The norms and seminorms of the Sobolev spaces $W^{k,p}(G)$, $k \in \mathbb{R}$, $p > 0$ are denoted by $\|\cdot\|_{k,p,G}$ and $|\cdot|_{k,p,G}$, respectively. The norms and seminorms of the Hilbert spaces $H^k(G)$ are denoted by $\|\cdot\|_{k,G}$ and $|\cdot|_{k,G}$, respectively. We omit G in the subscript if $G = \Omega$. For a section of the domain or element boundary $S \subset \mathbb{R}^{d-1}$ we write $\langle\cdot,\cdot\rangle_S$ and $\|\cdot\|_S$ for the $L^2(S)$ inner product (or duality pairing) and norm, respectively. We will also use the spaces

$$H(\operatorname{div}; \Omega) = \{v \in L^2(\Omega, \mathbb{R}^d) : \operatorname{div} v \in L^2(\Omega)\},$$
$$H(\operatorname{div}; \Omega, \mathbb{M}) = \{\tau \in L^2(\Omega, \mathbb{M}) : \operatorname{div} \tau \in L^2(\Omega, \mathbb{R}^d)\},$$

equipped with the norm

$$\|\tau\|_{\operatorname{div}} = \left(\|\tau\|^2 + \|\operatorname{div}\tau\|^2\right)^{1/2}.$$

We next present the mixed weak formulation, which has been proposed in [25]. Using (2.1) and (2.2), we have

$$\operatorname{div} u = \operatorname{tr}(\epsilon(u)) = \operatorname{tr}(A\sigma_e) = \operatorname{tr} A(\sigma + \alpha p I),$$

which can be substituted in (2.5) to give

$$\partial_t(c_0 p + \alpha \operatorname{tr} A(\sigma + \alpha p I)) + \operatorname{div} z = q,$$

where ∂_t is a short notation for $\frac{\partial}{\partial t}$. In the weakly symmetric stress formulation, we allow for σ to be non-symmetric and introduce the Lagrange multiplier $\gamma = \operatorname{Skew}(\nabla u)$, $\operatorname{Skew}(\tau) = \frac{1}{2}(\tau - \tau^T)$, from the space of skew-symmetric matrices. The constitutive equation (2.1) can be rewritten as

$$A(\sigma + \alpha p I) = \nabla u - \gamma.$$

The mixed weak formulation of the Biot problem reads: find $(\sigma, u, \gamma, z, p) : [0,T] \mapsto \mathbb{X} \times V \times \mathbb{Q} \times Z \times W$ such that $p(0) = p_0$ and, for a.e. $t \in (0,T)$,

$$(A(\sigma + \alpha p I), \tau) + (u, \operatorname{div}\tau) + (\gamma, \tau) = \langle g_u, \tau n\rangle_{\Gamma_D^{displ}}, \qquad \forall \tau \in \mathbb{X}, \tag{2.8}$$

$$(\operatorname{div}\sigma, v) = -(f, v), \qquad \forall v \in V, \tag{2.9}$$

$$(\sigma, \xi) = 0, \qquad \forall \xi \in \mathbb{Q}, \tag{2.10}$$

$$\left(K^{-1}z, \zeta\right) - (p, \operatorname{div}\zeta) = -\langle g_p, \zeta \cdot n\rangle_{\Gamma_D^{pres}}, \qquad \forall \zeta \in Z, \tag{2.11}$$

$$(c_0 \partial_t p, w) + \alpha\,(\partial_t A(\sigma + \alpha p I), wI) + (\operatorname{div} z, w) = (q, w), \qquad \forall w \in W, \tag{2.12}$$

where we have used the identity $(\operatorname{tr} A\tau, w) = (A\tau, wI)$ and the functional spaces are defined as

$$\mathbb{X} = \left\{\tau \in H(\operatorname{div}; \Omega, \mathbb{M}) : \tau n = 0 \text{ on } \Gamma_N^{stress}\right\}, \quad V = L^2(\Omega, \mathbb{R}^d), \quad \mathbb{Q} = L^2(\Omega, \mathbb{N}),$$
$$Z = \left\{\zeta \in H(\operatorname{div}; \Omega, \mathbb{R}^d) : \zeta \cdot n = 0 \text{ on } \Gamma_N^{vel}\right\}, \quad W = L^2(\Omega).$$

We refer the reader to [46] for the analysis of the well-posedness of a related displacement–pressure weak formulation. In Section 4 we establish existence, uniqueness, and stability for the semidiscrete continuous-in-time approximation of (2.8)–(2.12). The arguments there also apply to the weak formulation (2.8)–(2.12) itself. We make a remark here on the initial data $p_0(x)$. In particular, we assume that

$$p_0 \in H^1(\Omega), \quad p_0(x) = g_p(x,0) \text{ on } \Gamma_D^{pres}, \quad \text{and} \quad K\nabla p_0 \in Z. \tag{2.13}$$

A similar assumption is also made in [46]. In our case, we can set $z_0 = -K\nabla p_0 \in Z$ and show that it satisfies (2.11). We can also determine σ_0, u_0, and γ_0 by solving the elasticity problem (2.8)–(2.10) with p_0 given as data. We refer to the initial data obtained by this procedure as compatible initial data. It is needed for the well posedness of the (2.8)–(2.12), as we will discuss in Section 4.

3. Mixed finite element discretization

We begin with the discretization of the fully mixed weak formulation of the poroelasticity system (2.8)–(2.12), based on mixed finite element methods for elasticity and Darcy flow. We then present the multipoint stress–multipoint flux mixed finite element method, which employs the vertex quadrature rule for the stress, rotation, and velocity bilinear forms and can be reduced to a positive definite cell centered system for displacement and pressure only.

3.1. Mixed finite element spaces

We next present the MFE discretization of (2.8)–(2.12). For simplicity, assume that Ω is a polygonal domain. Let $\mathcal{T}_h$ be a shape-regular and quasi-uniform [14] finite element partition of Ω, consisting of triangles and/or quadrilaterals in two dimensions and tetrahedra in three dimensions. Let $h = \max_{E\in\mathcal{T}_h} \text{diam}(E)$. For any element $E \in \mathcal{T}_h$ there exists a bijection mapping $F_E : \hat{E} \to E$, where $\hat{E}$ is a reference element. We denote the Jacobian matrix by DF_E and let $J_E = |\det(DF_E)|$. We note that the mapping is affine with constant DF_E in the case of simplicial elements and bilinear with linear DF_E in the case of quadrilaterals. The shape-regularity and quasiuniformity of the grids imply that

$$\|DF_E\|_{0,\infty,\hat{E}} \sim h, \quad \|J_E\|_{0,\infty,\hat{E}} \sim h^d \quad \forall E \in \mathcal{T}_h. \tag{3.1}$$

Let $\mathbb{X}_h \times V_h \times \mathbb{Q}_h$ be the triple $(\mathcal{BDM}_1)^d \times (\mathcal{P}_0)^d \times \left(\mathcal{P}_1^{cts}\right)^{d\times d,skew}$ on simplicial elements or $(\mathcal{BDM}_1)^2 \times (\mathcal{Q}_0)^2 \times \left(\mathcal{Q}_1^{cts}\right)^{2\times 2,skew}$ on quadrilaterals, where $\mathcal{P}_k$ denotes the space of polynomials of total degree k and $\mathcal{Q}_k$ denotes the space of polynomials of degree k in each variable. This triple has been shown to be inf–sup stable for mixed elasticity with weak stress symmetry in [9,10,16] on simplices, in [26] on rectangles, and in [2] on quadrilaterals; see also related spaces with constant rotations on simplices [7] and quadrilaterals [5]. For the Darcy flow discretization we consider $Z_h \times W_h$ to be the lowest order $\mathcal{BDM}_1 \times \mathcal{P}_0$ MFE spaces [11,12,33]. On the reference simplex, these spaces are defined as

$$\hat{\mathbb{X}}(\hat{E}) = \left(\mathcal{P}_1(\hat{E})^d\right)^d, \qquad \hat{V}(\hat{E}) = \mathcal{P}_0(\hat{E})^d, \qquad \hat{\mathbb{Q}}(\hat{E}) = \mathcal{P}_1(\hat{E})^{d\times d,skew}, \tag{3.2}$$

$$\hat{Z}(\hat{E}) = \mathcal{P}_1(\hat{E})^d, \qquad \hat{W}(\hat{E}) = \mathcal{P}_0(\hat{E}). \tag{3.3}$$

On the reference square, the spaces are defined as

$$\begin{aligned}
\hat{\mathbb{X}}(\hat{E}) &= \left(\mathcal{P}_1(\hat{E})^2 + r\,\text{curl}\,(\hat{x}^2\hat{y}) + s\,\text{curl}\,(\hat{x}\hat{y}^2)\right)^2 \\
&= \begin{pmatrix} \alpha_1\hat{x} + \beta_1\hat{y} + \gamma_1 + r_1\hat{x}^2 + 2s_1\hat{x}\hat{y} & \alpha_2\hat{x} + \beta_2\hat{y} + \gamma_2 - 2r_1\hat{x}\hat{y} - s_1\hat{y}^2 \\ \alpha_3\hat{x} + \beta_3\hat{y} + \gamma_3 + r_2\hat{x}^2 + 2s_2\hat{x}\hat{y} & \alpha_4\hat{x} + \beta_4\hat{y} + \gamma_4 - 2r_2\hat{x}\hat{y} - s_2\hat{y}^2 \end{pmatrix}, \\
\hat{V}(\hat{E}) &= \mathcal{P}_0(\hat{E})^d, \quad \hat{\mathbb{Q}}(\hat{E}) = \mathcal{Q}_1(\hat{E})^{2\times 2,skew}, \\
\hat{Z}(\hat{E}) &= \mathcal{P}_1(\hat{E})^2 + r\,\text{curl}\,(\hat{x}^2\hat{y}) + s\,\text{curl}\,(\hat{x}\hat{y}^2) = \begin{pmatrix} \alpha_5\hat{x} + \beta_5\hat{y} + \gamma_5 + r_3\hat{x}^2 + 2s_3\hat{x}\hat{y} \\ \alpha_6\hat{x} + \beta_6\hat{y} + \gamma_6 - 2r_3\hat{x}\hat{y} - s_3\hat{y}^2 \end{pmatrix}, \\
\hat{W}(\hat{E}) &= \mathcal{P}_0(\hat{E}).
\end{aligned} \tag{3.4}$$

These spaces satisfy

$$\operatorname{div}\hat{\mathbb{X}}(\hat{E}) = \hat{V}(\hat{E}),\ \operatorname{div}\hat{Z}(\hat{E}) = \hat{W}(\hat{E});\ \ \forall\hat{\tau}\in\hat{\mathbb{X}}(\hat{E}),\ \forall\hat{\zeta}\in\hat{Z}(\hat{E}),\ \forall\hat{e}\in\partial\hat{E},\ \ \hat{\tau}\,\hat{n}_{\hat{e}}\in\mathcal{P}_1(\hat{e})^d,\ \hat{\zeta}\cdot\hat{n}_{\hat{e}}\in\mathcal{P}_1(\hat{e}).$$

It is known [11,12] that the degrees of freedom for $\mathcal{BDM}_1$ can be chosen to be the values of the normal fluxes at any two points on each edge $\hat{e}$ of $\hat{E}$ in 2d or any three points on each face $\hat{e}$ of $\hat{E}$ in 3d; similarly for the normal stresses in the case of $(\mathcal{BDM}_1)^d$. Here we choose these points to be at the vertices of $\hat{e}$ for both the velocity and stress spaces. This choice is motivated by the use of the vertex quadrature rule introduced in the next section.

To define the above spaces on any physical element $E\in\mathcal{T}_h$, the following transformations are used

$$\tau \overset{\mathcal{P}}{\leftrightarrow} \hat{\tau} : \tau^T = \frac{1}{J_E} DF_E\hat{\tau}^T\circ F_E^{-1}, \qquad v\leftrightarrow\hat{v} : v = \hat{v}\circ F_E^{-1}, \qquad \xi\leftrightarrow\hat{\xi} : \xi = \hat{\xi}\circ F_E^{-1},$$
$$\zeta \overset{\mathcal{P}}{\leftrightarrow} \hat{\zeta} : \zeta = \frac{1}{J_E} DF_E\hat{\zeta}\circ F_E^{-1}, \qquad w\leftrightarrow\hat{w} : w = \hat{w}\circ F_E^{-1},$$

for $\tau\in\mathbb{X}$, $v\in V$, $\xi\in\mathbb{Q}$, $\zeta\in Z$ and $w\in W$. The velocity vector and stress tensor are mapped by the Piola transformation, where the stress is transformed row-wise. The Piola transformation preserves the normal components and the divergence of the stress and velocity on element edges or faces. In particular, it can be shown that

$$\tau\, n_e = \frac{1}{|J_E DF^{-T}\hat{n}_{\hat{e}}|_{\mathbb{R}^d}}\hat{\tau}\,\hat{n}_{\hat{e}}, \quad \zeta\cdot n_e = \frac{1}{|J_E DF^{-T}\hat{n}_{\hat{e}}|_{\mathbb{R}^d}}\hat{\zeta}\cdot\hat{n}_{\hat{e}}, \quad \operatorname{div}\tau = \frac{1}{J_E}\operatorname{div}\hat{\tau}, \quad \operatorname{div}\zeta = \frac{1}{J_E}\operatorname{div}\hat{\zeta}, \tag{3.5}$$

where $|\cdot|_{\mathbb{R}^d}$ denotes the Euclidean vector norm. The finite element spaces on $\mathcal{T}_h$ are defined as

$$\begin{aligned}
\mathbb{X}_h &= \{\tau\in\mathbb{X} : \tau|_E \overset{\mathcal{P}}{\leftrightarrow}\hat{\tau},\ \hat{\tau}\in\hat{\mathbb{X}}(\hat{E}) \quad \forall E\in\mathcal{T}_h\},\\
V_h &= \{v\in V : v|_E\leftrightarrow\hat{v},\ \hat{v}\in\hat{V}(\hat{E}) \quad \forall E\in\mathcal{T}_h\},\\
\mathbb{Q}_h &= \{\xi\in H^1(\Omega,\mathbb{N}) : \xi|_E\leftrightarrow\hat{\xi},\ \hat{\xi}\in\hat{\mathbb{Q}}(\hat{E}) \quad \forall E\in\mathcal{T}_h\},\\
Z_h &= \{\zeta\in Z : \zeta|_E \overset{\mathcal{P}}{\leftrightarrow}\hat{\zeta},\ \hat{\zeta}\in\hat{Z}(\hat{E}) \quad \forall E\in\mathcal{T}_h\},\\
W_h &= \{w\in W : w|_E\leftrightarrow\hat{w},\ \hat{w}\in\hat{W}(\hat{E}) \quad \forall E\in\mathcal{T}_h\}.
\end{aligned} \tag{3.6}$$

Remark 3.1. Due to (3.5), on each $E\in\mathcal{T}_h$, it holds that $\operatorname{div}\mathbb{X}_h = \frac{1}{J_E}V_h$ and $\operatorname{div}Z_h = \frac{1}{J_E}W_h$. In several places we will make choices for test functions, on each E, $v = J_E\operatorname{div}\tau$ or $w = J_E\operatorname{div}\zeta$. On quadrilaterals, J_E is linear and positive. On simplices, J_E is a positive constant, so in this case $\operatorname{div}\mathbb{X}_h = V_h$ and $\operatorname{div}Z_h = W_h$.

3.2. The coupled $\mathcal{BDM}_1$ mixed finite element method

With the finite element spaces defined above, the semidiscrete five-field mixed finite element approximation of the Biot poroelasticity system (2.8)–(2.12) reads as follows: find $(\sigma_h, u_h, \gamma_h, z_h, p_h) : [0,T]\mapsto\mathbb{X}_h\times V_h\times\mathbb{Q}_h\times Z_h\times W_h$ such that, for a.e. $t\in(0,T)$,

$$(A(\sigma_h+\alpha p_h I),\tau) + (u_h,\operatorname{div}\tau) + (\gamma_h,\tau) = \langle g_u,\tau\,n\rangle_{\Gamma_D^{displ}}, \qquad \forall\tau\in\mathbb{X}_h, \tag{3.7}$$
$$(\operatorname{div}\sigma_h, v) = -(f,v), \qquad \forall v\in V_h, \tag{3.8}$$
$$(\sigma_h,\xi) = 0, \qquad \forall\xi\in\mathbb{Q}_h, \tag{3.9}$$
$$\left(K^{-1}z_h,\zeta\right) - (p_h,\operatorname{div}\zeta) = -\langle g_p,\zeta\cdot n\rangle_{\Gamma_D^{pres}}, \qquad \forall\zeta\in Z_h, \tag{3.10}$$
$$(c_0\partial_t p_h, w) + \alpha\,(\partial_t A(\sigma_h+\alpha p_h I), wI) + (\operatorname{div} z_h, w) = (q,w), \qquad \forall w\in W_h, \tag{3.11}$$

with initial condition $p_h(0) = p_{h,0}$, where $p_{h,0}$ is a suitable approximation of p_0. The convergence of the above method is studied in [25], where it is shown that the method is robust for small storage coefficient and for nearly incompressible materials. With an implicit time discretization, it requires the solution of a large five-field saddle point system at each time step, which is computationally expensive. Motivated by the MFMFE [52] and MSMFE [2,3] methods, in the next sections we develop a coupled MSMFE–MFMFE method based on a vertex quadrature rule that allows for local elimination of the stress, rotation, and velocity without loss of accuracy, resulting in a significantly more efficient positive-definite cell-centered displacement–pressure system.

3.3. A quadrature rule

For any element-wise continuous vector or tensor functions ϕ and ψ on Ω, we denote by

$$(\varphi, \psi)_Q = \sum_{E \in \mathcal{T}_h} (\varphi, \psi)_{Q,E}$$

the application of the element-wise vertex quadrature rule for computing (φ, ψ). The integration on any element E is performed by mapping to the reference element $\hat{E}$. Let $\tilde{\phi}$ and $\tilde{\psi}$ be the mapped functions on $\hat{E}$, using the standard change of variables. Since $(\phi, \psi)_E = (\tilde{\phi}, \tilde{\psi} J_E)_{\hat{E}}$, we define

$$(\phi, \psi)_{Q,E} = \frac{|\hat{E}|}{s} \sum_{i=1}^{s} \tilde{\phi}(\hat{\mathbf{r}}_i) \cdot \tilde{\psi}(\hat{\mathbf{r}}_i) J_E(\hat{\mathbf{r}}_i) = \frac{|\hat{E}|}{s} \sum_{i=1}^{s} \phi(\mathbf{r}_i) \cdot \psi(\mathbf{r}_i) J_E(\hat{\mathbf{r}}_i),$$

where s is the number of vertices of E, $\mathbf{r}_i$ and $\hat{\mathbf{r}}_i$, $i = 1, \ldots, s$, are the vertices of E and $\hat{E}$, respectively, and $\cdot$ has a meaning of inner product for both vector and tensor valued functions.

The quadrature rule will be applied to the velocity, stress, and stress–rotation bilinear forms. All three variables have degrees of freedom associated with the mesh vertices. The quadrature rule decouples degrees of freedom associated with a vertex from the rest of the degrees of freedom, resulting in block-diagonal matrices corresponding to these bilinear forms. Therefore the velocity, stress, and rotation can be locally eliminated, reducing the method to solving a cell-centered pressure–displacement system. More details on this reduction will be provided in the following sections.

The analysis of the MSMFE–MFMFE method will utilize the following continuity and coercivity properties of the quadrature bilinear forms.

Lemma 3.1. *There exist positive constants C_1 and C_2 independent of h, such that for any linear uniformly bounded and positive-definite operator L and for all $\phi, \psi \in \mathbb{X}_h, \mathbb{Q}_h, Z_h, W_h$,*

$$(L\phi, \phi)_Q \geq C_1 \|\phi\|^2, \quad (L\phi, \psi)_Q \leq C_2 \|\phi\| \|\psi\|. \tag{3.12}$$

Proof. The proof for functions in $\mathbb{X}_h, \mathbb{Q}_h, Z_h$ has been shown in [2,3,52]. The proof for functions in W_h is similar. □

Lemma 3.1 implies the following norm equivalence.

Corollary 3.1. *$(L\phi, \phi)_Q^{1/2}$ is a norm equivalent to $\|\phi\|$, which will be denoted by $\|L^{1/2}\phi\|_Q$.*

3.4. The coupled multipoint stress–multipoint flux mixed finite element method

We first note that there is a slight difference in the incorporation of the Dirichlet boundary conditions between the simplicial and quadrilateral grids. In particular, in the case of quadrilaterals, the L^2 projection of the boundary data onto the space of piecewise constants must be used in order to obtain optimal approximation of the boundary term. On the other hand, such projection should not be used on simplices, since it would result in non-optimal approximation. The difference is due to different properties of the quadrature rules on simplicial and quadrilateral grids, see [2,3,51]. For the conformity and simplicity of the presentation, for the rest of the paper we consider $g_u = g_p = 0$.

Our method, referred to as the MSMFE–MFMFE method, in its semidiscrete form is defined as follows: find $(\sigma_h, u_h, \gamma_h, z_h, p_h) : [0, T] \mapsto \mathbb{X}_h \times V_h \times \mathbb{Q}_h \times Z_h \times W_h$ such that $p_h(0) = p_{h,0}$ and, for a.e. $t \in (0, T)$,

$$(A(\sigma_h + \alpha p_h I), \tau)_Q + (u_h, \operatorname{div} \tau) + (\gamma_h, \tau)_Q = 0, \qquad \forall \tau \in \mathbb{X}_h, \tag{3.13}$$

$$(\operatorname{div} \sigma_h, v) = -(f, v), \qquad \forall v \in V_h, \tag{3.14}$$

$$(\sigma_h, \xi)_Q = 0, \qquad \forall \xi \in \mathbb{Q}_h, \tag{3.15}$$

$$\left(K^{-1} z_h, \zeta\right)_Q - (p_h, \operatorname{div} \zeta) = 0, \qquad \forall \zeta \in Z_h, \tag{3.16}$$

$$(c_0 \partial_t p_h, w) + \alpha (\partial_t A(\sigma_h + \alpha p_h I), w I)_Q + (\operatorname{div} z_h, w) = (q, w), \qquad \forall w \in W_h. \tag{3.17}$$

Remark 3.2. We note that the quadrature rule is employed for both $(A(\sigma_h + \alpha p_h I), \tau)_Q$ in (3.13) and $\alpha\,(\partial_t A(\sigma_h + \alpha p_h I), wI)_Q$ in (3.17), since these two terms will be combined to obtain a coercive term in the well-posedness analysis, while only quadrature rule on the stress term $(A\sigma_h, \tau)_Q$ in (3.13) is needed for local stress elimination.

In the next sections we proceed with establishing existence, uniqueness, stability, and error analysis for the semidiscrete MSMFE–MFMFE method (3.13)–(3.17). In Section 7 we present the fully-discrete MSMFE–MFMFE method and discuss the reduction of the algebraic system at each time step to a positive definite cell-centered displacement–pressure system.

4. Existence and uniqueness for the semidiscrete MSMFE–MFMFE method

We first state the inf–sup stability of the mixed Darcy and elasticity spaces, which will be utilized in the analysis. It is known [11] that the spaces $Z_h \times W_h$ satisfy the inf–sup condition

$$\exists\, \beta_1 > 0 \text{ such that } \forall\, w_h \in W_h, \quad \sup_{0\neq\zeta\in Z_h} \frac{(w_h, \operatorname{div}\zeta)}{\|\zeta\|_{\operatorname{div}}} \geq \beta_1 \|w_h\|. \tag{4.1}$$

The inf–sup stability for the mixed elasticity spaces $\mathbb{X}_h \times V_h \times \mathbb{Q}_h$ with quadrature has been studied in [3] on simplices and in [2] on quadrilaterals. In the case of quadrilaterals, the following assumptions on the grid are needed [2]:

(M1) Each element E has at most one edge on Γ_N^{stress},

(M2) The mesh size h is sufficiently small and there exists a constant C such that for every pair of neighboring elements E and $\tilde{E}$ such that E or $\tilde{E}$ is a non-parallelogram, and every pair of edges $e \subset \partial E \backslash \partial\tilde{E}$, $\tilde{e} \subset \partial\tilde{E} \backslash \partial E$ that share a vertex,

$$|\mathbf{r}_e - \mathbf{r}_{\tilde{e}}|_{\mathbb{R}^2} \leq Ch^2,$$

where $\mathbf{r}_e$ and $\mathbf{r}_{\tilde{e}}$ are the vectors corresponding to e and $\tilde{e}$, respectively.

We note that **(M2)** can be thought of as a smoothness assumption on the grid and it is not needed if the grid consists entirely of parallelograms. For the rest of the paper we will tacitly assume that **(M1)**–**(M2)** hold on quadrilaterals.

We have the following inf–sup condition on simplices [3] and quadrilaterals [2]:

$$\exists\, \beta_2 > 0 \text{ such that } \forall\, v_h \in V_h,\ \xi_h \in \mathbb{Q}_h, \quad \sup_{0\neq\tau\in\mathbb{X}_h} \frac{(v_h, \operatorname{div}\tau) + (\xi_h, \tau)_Q}{\|\tau\|_{\operatorname{div}}} \geq \beta_2(\|v_h\| + \|\xi_h\|). \tag{4.2}$$

We note that the semidiscrete method (3.13)–(3.17) is a system of differential–algebraic equations and the standard theory for ordinary differential equations cannot be directly applied. Instead, the well posedness analysis of (3.13)–(3.17) will be based on the existence theory for degenerate parabolic systems, in particular [48, Theorem 6.1(b)].

Theorem 4.1. *Let the linear, symmetric and monotone operator $\mathcal{N}$ be given for the real vector space E to its algebraic dual E^*, and let E_b' be the Hilbert space which is the dual of E with the seminorm*

$$|x|_b \;=\; (\mathcal{N}x\,(x))^{1/2}\,, \quad x \in E.$$

Let $\mathcal{M} \subset E \times E_b'$ be a relation with domain $D = \{x \in E : \mathcal{M}(x) \neq \emptyset\}$. Assume $\mathcal{M}$ is monotone and $Rg(\mathcal{N} + \mathcal{M}) = E_b'$. Then, for each $x_0 \in D$ and for each $\mathcal{F} \in W^{1,1}(0, T; E_b')$, there is a solution x of

$$\frac{\partial}{\partial t}\,(\mathcal{N}x(t)) + \mathcal{M}\,(x(t)) \ni \mathcal{F}(t)\,, \quad a.e.\ \ 0 < t < T, \tag{4.3}$$

with

$$\mathcal{N}x \in W^{1,\infty}(0, T; E_b')\,,\ \ x(t) \in D\,,\ \text{for all } 0 \leq t \leq T\,,\ \ \text{and}\ \ \mathcal{N}x(0) = \mathcal{N}x_0\,.$$

Theorem 4.2. *For each $f \in W^{1,\infty}(0, T; L^2(\Omega))$, $q \in W^{1,\infty}(0, T; L^2(\Omega))$, and compatible initial data $(\sigma_{h,0}, u_{h,0}, \gamma_{h,0}, z_{h,0}, p_{h,0})$, the semidiscrete MSMFE–MFMFE method (3.13)–(3.17) has a unique solution $(\sigma_h, u_h, \gamma_h, z_h, p_h) \in W^{1,\infty}(0, T; L^2(\Omega, \mathbb{M})) \cap L^\infty(0, T; \mathbb{X}_h) \times L^\infty(0, T; V_h) \times L^\infty(0, T; \mathbb{Q}_h) \times L^\infty(0, T; Z_h) \times W^{1,\infty}(0, T; W_h)$.*

Proof. In order to fit (3.13)–(3.17) in the form of Theorem 4.1, we consider a slightly modified formulation, with (3.13) differentiated in time and the new variables $\dot{u}_h$ and $\dot{\gamma}_h$ representing $\partial_t u_h$ and $\partial_t \gamma_h$, respectively:

$$(\partial_t A(\sigma_h + \alpha p_h I), \tau)_Q + (\dot{u}_h, \operatorname{div} \tau) + (\dot{\gamma}_h, \tau)_Q = 0, \quad \forall \tau \in \mathbb{X}_h. \tag{4.4}$$

Introducing the operators

$$(A_{\sigma\sigma}\sigma_h, \tau) = (A\sigma_h, \tau)_Q\,,\ (A_{\sigma p}\sigma_h, w) = \alpha\,(A\sigma_h, wI)_Q\,,\ (A_{\sigma u}\sigma_h, v) = (\operatorname{div}\sigma_h, v)\,,\ (A_{\sigma\gamma}\sigma_h, \xi) = (\sigma_h, \xi)_Q\,,$$
$$(A_{zz}\zeta_h, \zeta) = \left(K^{-1}z_h, \zeta\right)_Q\,,\quad (A_{zp}\zeta_h, w) = -\,(\operatorname{div} z_h, w)\,,\quad (A_{pp}p_h, w) = (c_0 p_h, w) + \alpha\,(A\alpha p_h I, wI)_Q\,,$$

we have a system in the form of (4.3), where

$$\dot{x} = \begin{pmatrix} \sigma_h \\ \dot{u}_h \\ \dot{\gamma}_h \\ z_h \\ p_h \end{pmatrix},\ \mathcal{N} = \begin{pmatrix} A_{\sigma\sigma} & 0 & 0 & 0 & A_{\sigma p}^T \\ 0 & 0 & 0 & 0 & 0 \\ 0 & 0 & 0 & 0 & 0 \\ 0 & 0 & 0 & 0 & 0 \\ A_{\sigma p} & 0 & 0 & 0 & A_{pp} \end{pmatrix},\ \mathcal{M} = \begin{pmatrix} 0 & A_{\sigma u}^T & A_{\sigma\gamma}^T & 0 & 0 \\ -A_{\sigma u} & 0 & 0 & 0 & 0 \\ -A_{\sigma\gamma} & 0 & 0 & 0 & 0 \\ 0 & 0 & 0 & A_{zz} & A_{zp}^T \\ 0 & 0 & 0 & -A_{zp} & 0 \end{pmatrix},\ \mathcal{F} = \begin{pmatrix} 0 \\ -f \\ 0 \\ 0 \\ q \end{pmatrix}.$$

The dual space E_b' is $L^2(\Omega, \mathbb{M}) \times 0 \times 0 \times 0 \times L^2(\Omega)$, and the condition $\mathcal{F} \in W^{1,1}(0, T; E_b')$ in Theorem 4.1 allows for non-zero source terms only in the equations with time derivatives. In our case this means $f = 0$. We can reduce our problem to a system with $f = 0$ by solving for each $t \in (0, T]$ an elasticity problem with a source term f, cf. [47] for a similar approach:

$$\begin{pmatrix} A_{\sigma\sigma} & A_{\sigma u}^T & A_{\sigma\gamma}^T \\ -A_{\sigma u} & 0 & 0 \\ -A_{\sigma\gamma} & 0 & 0 \end{pmatrix} \begin{pmatrix} \sigma_h^f \\ \dot{u}_h^f \\ \dot{\gamma}_h^f \end{pmatrix} = \begin{pmatrix} 0 \\ -f \\ 0 \end{pmatrix},$$

and subtracting this solution from the solution to (3.13)–(3.17), resulting in a problem with a modified right hand side $\mathcal{F} = (A_{\sigma\sigma}(\sigma_h^f - \partial_t \sigma_h^f), 0, 0, 0, q - A_{\sigma p}\partial_t \sigma_h^f)^T$.

The range condition $Rg(\mathcal{N} + \mathcal{M}) = E_b'$ can be verified by showing that the square finite dimensional homogeneous system: find $(\hat{\sigma}_h, \hat{u}_h, \hat{\gamma}_h, \hat{z}_h, \hat{p}_h) \in \mathbb{X}_h \times V_h \times \mathbb{Q}_h \times Z_h \times W_h$ such that

$$\left(A(\hat{\sigma}_h + \alpha \hat{p}_h I), \tau\right)_Q + \left(\hat{u}_h, \operatorname{div}\tau\right) + \left(\hat{\gamma}_h, \tau\right)_Q = 0, \qquad \forall \tau \in \mathbb{X}_h, \tag{4.5}$$
$$\left(\operatorname{div}\hat{\sigma}_h, v\right) = 0, \qquad \forall v \in V_h, \tag{4.6}$$
$$\left(\hat{\sigma}_h, \xi\right)_Q = 0, \qquad \forall \xi \in \mathbb{Q}_h, \tag{4.7}$$
$$\left(K^{-1}\hat{z}_h, \zeta\right)_Q - \left(\hat{p}_h, \operatorname{div}\zeta\right) = 0, \qquad \forall \zeta \in Z_h, \tag{4.8}$$
$$\left(c_0\hat{p}_h, w\right) + \alpha\left(A(\hat{\sigma}_h + \alpha\hat{p}_h I), wI\right)_Q + \left(\operatorname{div}\hat{z}_h, w\right) = 0, \qquad \forall w \in W_h, \tag{4.9}$$

has only the zero solution, see also [25, Section 3.4]. Taking $(\tau, v, \xi, \zeta, w) = (\hat{\sigma}_h, \hat{u}_h, \hat{\gamma}_h, \hat{z}_h, \hat{p}_h)$ and combining the equations implies $\|A^{1/2}(\hat{\sigma}_h + \alpha\hat{p}_h I)\|_Q^2 + \|c_0^{1/2}\hat{p}_h\|^2 + \|K^{-1/2}\hat{z}_h\|_Q^2 = 0$, which gives $\hat{\sigma}_h + \alpha\hat{p}_h I = 0$ and $\hat{z}_h = 0$, using the positive definiteness of A and K and the coercivity (3.12). Then the Darcy inf–sup condition (4.1) implies that $\hat{p}_h = 0$, and therefore $\hat{\sigma}_h = 0$. The elasticity inf–sup condition (4.2) now implies that $\hat{u}_h = 0$ and $\hat{\gamma}_h = 0$.

The above argument can also be used to conclude that $\mathcal{N}$ and $\mathcal{M}$ are non-negative, and therefore, due to their linearity, monotone.

Finally, we need compatible initial data $\dot{x}_0 \in D$, i.e., $\mathcal{M}\dot{x}_0 \in E_b'$. Let us consider first initial data $x_0 = (\sigma_{h,0}, u_{h,0}, \gamma_{h,0}, z_{h,0}, p_{h,0})$ for the non-differentiated problem (3.13)–(3.17). We take x_0 to be the elliptic projection of the initial data $\tilde{x}_0 = (\sigma_0, u_0, \gamma_0, z_0, p_0)$ for the weak formulation (2.8)–(2.12), which is constructed from p_0 by the procedure described at the end of Section 2. With the reduction to a problem with $f = 0$, the construction satisfies $(\mathcal{N} + \mathcal{M})\tilde{x}_0 \in E_b'$. Since we have

$$(\mathcal{N} + \mathcal{M})x_0 = (\mathcal{N} + \mathcal{M})\tilde{x}_0, \tag{4.10}$$

this implies that $\mathcal{M}x_0 = (\mathcal{N} + \mathcal{M})\tilde{x}_0 - \mathcal{N}x_0 \in E_b'$. For the initial data of the differentiated problem (4.4),(3.14)–(3.17), we simply take $\dot{x}_0 = (\sigma_{h,0}, 0, 0, z_{h,0}, p_{h,0})$, which also satisfies $\mathcal{M}\dot{x}_0 \in E_b'$. We note that $u_{h,0}$ and $\gamma_{h,0}$ are not needed for the differentiated problem, but will be used to recover the solution of the original problem.

Now, all conditions of Theorem 4.1 are satisfied and we conclude the existence of a solution to (4.4), (3.14)–(3.17) with $\sigma_h \in W^{1,\infty}(0, T; L^2(\Omega, \mathbb{M})) \cap L^\infty(0, T; \mathbb{X}_h)$, $p_h \in W^{1,\infty}(0, T; W_h)$, $\sigma_h(0) = \sigma_{h,0}$, and $p_h(0) = p_{h,0}$.

From the equations we can further conclude that $\dot{u}_h \in L^\infty(0,T;V_h)$, $\dot{\gamma}_h \in L^\infty(0,T;\mathbb{Q}_h)$ and $z_h \in L^\infty(0,T;Z_h)$. By taking $t \to 0$ in (3.16) and using that $z_{h,0}$ and $p_{h,0}$ satisfy (3.16) at $t=0$, we also have that $z_h(0) = z_{h,0}$.

Next, we recover the solution of the original problem. Let us define

$$u_h(t) = u_{h,0} + \int_0^t \dot{u}_h ds, \quad \gamma_h(t) = \gamma_{h,0} + \int_0^t \dot{\gamma}_h ds, \quad \forall\, t \in [0,T]. \tag{4.11}$$

By construction, $u_h(0) = u_{h,0}$ and $\gamma_h(0) = \gamma_{h,0}$. Integrating (4.4) in time from 0 to any $t \in (0,T]$ and using that $\sigma_{h,0}$, $u_{h,0}$, and $\gamma_{h,0}$ satisfy (3.13) at $t=0$, we conclude that (3.13) holds for all t. This completes the existence proof. Uniqueness follows from the stability bound given in Theorem 5.1 in the next section. □

Remark 4.1. The above argument and the stability bound below do not require $c_0 > 0$, implying well posedness even for $c_0 = 0$.

5. Stability analysis of the semidiscrete MSMFE–MFMFE method

In this section we derive a stability bound for the MSMFE–MFMFE method (3.13)–(3.17). We remark that stability analysis for the $\mathcal{BDM}_1$ MFE method (3.7)–(3.11) was not performed in [25], where only error analysis was carried out. The stability analysis is more involved than the error analysis, since controlling the boundary condition term $\langle g_p, \zeta\cdot n\rangle_{\Gamma_D^{pres}}$ requires bounding $\|\operatorname{div} z_h\|$. Even though we consider $g_p = 0$, we derive a bound on $\|\operatorname{div} z_h\|$, thus obtaining full control on $\|z_h\|_{\operatorname{div}}$.

Theorem 5.1. *There exists a positive constant C independent of h and c_0, such that the solution of (3.13)–(3.17) satisfies*

$$\begin{aligned}
&\|\sigma_h\|_{L^\infty(0,T;H(\operatorname{div};\Omega))} + \|u_h\|_{L^\infty(0,T;L^2(\Omega))} + \|\gamma_h\|_{L^\infty(0,T;L^2(\Omega))} + \|z_h\|_{L^\infty(0,T;L^2(\Omega))} + \|p_h\|_{L^\infty(0,T;L^2(\Omega))} \\
&\quad + \|\sigma_h\|_{L^2(0,T;H(\operatorname{div};\Omega))} + \|u_h\|_{L^2(0,T;L^2(\Omega))} + \|\gamma_h\|_{L^2(0,T;L^2(\Omega))} + \|z_h\|_{L^2(0,T;H(\operatorname{div};\Omega))} + \|p_h\|_{L^2(0,T;L^2(\Omega))} \\
&\qquad \le C\left(\|f\|_{H^1(0,T;L^2(\Omega))} + \|q\|_{H^1(0,T;L^2(\Omega))} + \|p_0\|_{H^1(\Omega)} + \|K\nabla p_0\|_{H(\operatorname{div};\Omega)}\right).
\end{aligned} \tag{5.1}$$

Proof. We differentiate (3.13) in time, choose $(\tau, v, \xi, \zeta, w) = (\sigma_h, \partial_t u_h, \partial_t \gamma_h, z_h, p_h)$ in Eqs. (3.13)–(3.17), and combine them to obtain

$$(\partial_t(A\sigma_h + \alpha p_h I), \sigma_h + \alpha p_h I)_Q + (c_0 \partial_t p_h, p_h) + \left(K^{-1} z_h, z_h\right)_Q = (f, \partial_t u_h) + (q, p_h),$$

implying

$$\frac{1}{2}\partial_t\left[\|A^{1/2}(\sigma_h + \alpha p_h I)\|_Q^2 + \|c_0^{1/2} p_h\|^2\right] + \|K^{-1/2} z_h\|_Q^2 = (f, \partial_t u_h) + (q, p_h). \tag{5.2}$$

Next, integrating (5.2) in time from 0 to an arbitrary $t \in (0,T]$ results in

$$\begin{aligned}
&\frac{1}{2}\left[\|A^{1/2}(\sigma_h + \alpha p_h I)(t)\|_Q^2 + \|c_0^{1/2} p_h(t)\|^2\right] + \int_0^t \|K^{-1/2} z_h\|_Q^2\, ds \\
&\quad = \int_0^t ((q, p_h) - (\partial_t f, u_h))\, ds + \frac{1}{2}\left[\|A^{1/2}(\sigma_h + \alpha p_h I)(0)\|_Q^2 + \|c_0^{1/2} p_h(0)\|^2\right] + (f, u_h)(t) - (f, u_h)(0).
\end{aligned}$$

Applying the Cauchy–Schwartz and Young's inequalities, we obtain

$$\begin{aligned}
&\|A^{1/2}(\sigma_h + \alpha p_h I)(t)\|_Q^2 + \|c_0^{1/2} p_h(t)\|^2 + 2\int_0^t \|K^{-1/2} z_h\|_Q^2\, ds \\
&\quad \le \epsilon_1\left(\|u_h(t)\|^2 + \int_0^t (\|p_h\|^2 + \|u_h\|^2)\, ds\right) + \frac{1}{\epsilon_1}\left(\|f(t)\|^2 + \int_0^t \left(\|q\|^2 + \|\partial_t f\|^2\right) ds\right) \\
&\qquad + \|A^{1/2}(\sigma_h + \alpha p_h I)(0)\|_Q^2 + \|c_0^{1/2} p_h(0)\|^2 + \|u_h(0)\|^2 + \|f(0)\|^2.
\end{aligned} \tag{5.3}$$

Using the inf–sup condition (3.13) and (4.2), we bound $\|u_h\|$ and $\|\gamma_h\|$ as follows,

$$\begin{aligned}\|u_h\| + \|\gamma_h\| &\leq C \sup_{0\neq\tau\in\mathbb{X}_h} \frac{(u_h, \operatorname{div}\tau) + (\gamma_h, \tau)_Q}{\|\tau\|_{\operatorname{div}}} \\ &= C \sup_{0\neq\tau\in\mathbb{X}_h} \frac{-\left(A^{1/2}(\sigma_h + \alpha p_h I), A^{1/2}\tau\right)_Q}{\|\tau\|_{\operatorname{div}}} \leq C\|A^{1/2}(\sigma_h + \alpha p_h I)\|, \end{aligned} \tag{5.4}$$

where in the last step we used the equivalence of norms as stated in Corollary 3.1. We also note that

$$\int_0^t \left(\|u_h\|^2 + \|\gamma_h\|^2\right) ds \leq C \int_0^t \left(\|\sigma_h\|^2 + \|p_h\|^2\right) ds. \tag{5.5}$$

Similarly, using the inf–sup condition (3.16) and (4.1), we have

$$\|p_h\| \leq C \sup_{0\neq\zeta\in Z_h} \frac{(p_h, \operatorname{div}\zeta)}{\|\zeta\|_{\operatorname{div}}} = C \sup_{0\neq\zeta\in Z_h} \frac{\left(K^{-1}z_h, \zeta\right)_Q}{\|\zeta\|_{\operatorname{div}}} \leq C\|K^{-1/2}z_h\|. \tag{5.6}$$

To obtain a bound on $\int_0^t \|\sigma_h\|^2 ds$, which appears on the right hand side of (5.5), we take $\tau = \sigma_h$, $v = u_h$, $\xi = \gamma_h$ in (3.13)–(3.15), and use Cauchy–Schwartz and Young's inequalities, to obtain

$$\|\sigma_h\|^2 \leq C\Big(\|p_h\|^2 + \epsilon_2\|u_h\|^2 + \frac{1}{\epsilon_2}\|f\|^2\Big). \tag{5.7}$$

Also, testing (3.14) with $v = J_E \operatorname{div}\sigma_h$ on each $E \in \mathcal{T}_h$, we obtain a bound on the stress divergence:

$$\|\operatorname{div}\sigma_h\| \leq \|f\|. \tag{5.8}$$

Combining inequalities (5.3)–(5.8) and choosing ϵ_2 small enough, then ϵ_1 small enough, we obtain

$$\begin{aligned}&\|A^{1/2}(\sigma_h + \alpha p_h I)(t)\|^2 + \|u_h(t)\|^2 + \|\gamma_h(t)\|^2 + \|c_0^{1/2}p_h(t)\|^2 + \|\operatorname{div}\sigma_h(t)\|^2 \\ &\quad + \int_0^t \left(\|\sigma_h\|^2 + \|u_h\|^2 + \|\gamma_h\|^2 + \|K^{-1/2}z_h\|^2 + \|p_h\|^2 + \|\operatorname{div}\sigma_h\|^2\right) ds \\ &\leq C\Big(\|f(t)\|^2 + \int_0^t \left(\|q\|^2 + \|f\|^2 + \|\partial_t f\|^2\right) ds \\ &\qquad + \|\sigma_h(0)\|^2 + \|p_h(0)\|^2 + \|u_h(0)\|^2 + \|f(0)\|^2\Big). \end{aligned} \tag{5.9}$$

Estimate for $\operatorname{div} z_h$. We note that (5.9) is a self-contained stability estimate. We now proceed with obtaining a bound on $\|\operatorname{div} z_h\|$. In the process, we also obtain a bound on $\|K^{-1/2}z_h(t)\|$ for all t, and as a result, a bound on $\|p_h(t)\|$ for all t that is independent of c_0. We choose on each $E \in \mathcal{T}_h$, $w_h = J_E \operatorname{div} z_h$ in (3.17) and obtain

$$\|\operatorname{div} z_h\| \leq C\left(\|c_0^{1/2}\partial_t p_h\| + \|\partial_t A^{1/2}(\sigma_h + \alpha p_h I)\| + \|q\|\right). \tag{5.10}$$

To control the first two terms on the right hand side of (5.10), we differentiate Eqs. (3.13)–(3.16) in time and combine them with (3.17) as it was done in (5.2)–(5.3), with the choice $(\tau, v, \xi, \zeta, w) = (\partial_t\sigma_h, \partial_t u_h, \partial_t\gamma_h, z_h, \partial_t p_h)$, resulting in

$$\begin{aligned}&2\int_0^t \left(\|\partial_t A^{1/2}(\sigma_h + \alpha p_h I)\|_Q^2 + \|c_0^{1/2}\partial_t p_h\|^2\right) ds + \|K^{-1/2}z_h(t)\|_Q^2 \\ &\leq \epsilon\left(\|p_h(t)\|^2 + \int_0^t \|\partial_t u_h\|^2 ds\right) + \frac{1}{\epsilon}\left(\|q(t)\|^2 + \int_0^t \|\partial_t f\|^2 ds\right) \\ &\quad + \int_0^t \left(\|p_h\|^2 + \|\partial_t q\|^2\right) ds + \|K^{-1/2}z_h(0)\|_Q^2 + \|p_h(0)\|^2 + \|q(0)\|^2. \end{aligned} \tag{5.11}$$

Using the inf–sup condition (3.13) and (4.2), differentiated in time, we have

$$\|\partial_t u_h\| + \|\partial_t\gamma_h\| \leq C\|\partial_t A^{1/2}(\sigma_h + \alpha p_h I)\|. \tag{5.12}$$

Combining (5.11), (5.12), and (5.6), we get

$$\int_0^t \left(\|\partial_t A^{1/2}(\sigma_h + \alpha p_h I)\|^2 + \|\partial_t u_h\|^2 + \|\partial_t \gamma_h\|^2 + \|c_0^{1/2}\partial_t p_h\|^2 \right) ds + \|K^{-1/2} z_h(t)\|^2 + \|p_h(t)\|^2$$
$$\leq C \left(\int_0^t \left(\|p_h\|^2 + \|\partial_t q\|^2 + \|\partial_t f\|^2 \right) ds + \|q(t)\|^2 + \|z_h(0)\|^2 + \|p_h(0)\|^2 + \|q(0)\|^2 \right). \tag{5.13}$$

Integrating (5.10) in time and using (5.9) and (5.13), results in

$$\|K^{-1/2} z_h(t)\|^2 + \|p_h(t)\|^2 + \int_0^t \|\operatorname{div} z_h\|^2 ds$$
$$\leq C \Big(\|q(t)\|^2 + \|f(t)\|^2 + \int_0^t \left(\|q\|^2 + \|f\|^2 + \|\partial_t q\|^2 + \|\partial_t f\|^2 \right) ds$$
$$+ \|\sigma_h(0)\|^2 + \|p_h(0)\|^2 + \|u_h(0)\|^2 + \|z_h(0)\|^2 + \|q(0)\|^2 + \|f(0)\|^2 \Big). \tag{5.14}$$

We note that the control on $\|A^{1/2}(\sigma_h + \alpha p_h I)(t)\|$ and $\|p_h(t)\|$ also implies a bound on $\|\sigma_h(t)\|$:

$$\|\sigma_h\| \leq C(\|A^{1/2}(\sigma_h + \alpha p_h I)\| + \|p_h\|). \tag{5.15}$$

Finally, we recall the construction of the initial data $(\sigma_0, u_0, \gamma_0, z_0, p_0)$ for the weak formulation (2.8)–(2.12), see Section 2, and that the discrete initial data $(\sigma_{h,0}, u_{h,0}, \gamma_{h,0}, z_{h,0}, p_{h,0})$ is taken as its elliptic projection, see (4.10). Then following the steady-state version of the arguments presented in (5.2)–(5.15), we obtain

$$\|\sigma_h(0)\| + \|u_h(0)\| + \|\gamma_h(0)\| + \|p_h(0)\| + \|z_h(0)\| \leq C(\|\sigma_0\| + \|u_0\| + \|\gamma_0\| + \|p_0\| + \|z_0\|)$$
$$\leq C(\|p_0\|_{H^1(\Omega)} + \|K\nabla p_0\|_{H(\operatorname{div};\Omega)}). \tag{5.16}$$

The proof is completed by combining (5.9), (5.8), (5.14), (5.15), and (5.16). □

Remark 5.1. The constant in (5.1) does not depend on c_0, so we have stability even for $c_0 = 0$. Furthermore, since we did not use Gronwall's inequality in the proof, the constant also does not involve exponential growth in time, resulting in a long-time stability.

6. Error analysis

In this section we establish optimal order error estimates for all variables in their natural norms.

6.1. Preliminaries

We begin with several auxiliary results that will be used to bound the approximation and quadrature errors. Due to the reduced approximation properties of the MFE spaces on general quadrilaterals [6], we restrict the quadrilateral elements to be $O(h^2)$-perturbations of parallelograms:

$$\|\mathbf{r}_{34} - \mathbf{r}_{21}\| \leq Ch^2. \tag{6.1}$$

In this case it is easy to verify (see [52] for details) that

$$|DF_E|_{1,\infty,\hat{E}} \leq Ch^2 \quad \text{and} \quad \left| \frac{1}{J_E} DF_E \right|_{j,\infty,\hat{E}} \leq Ch^{j-1}, \ j = 1, 2. \tag{6.2}$$

Let $Q^0 : L^2(\Omega) \to W_h$ be a projection operator satisfying for any $\phi \in L^2(\Omega)$,

$$(\hat{Q}^0\hat{\phi} - \hat{\phi}, \hat{w})_{\hat{E}} = 0, \quad \forall\, \hat{w} \in \hat{W}(\hat{E}), \quad Q^0\phi = \hat{Q}^0\hat{\phi} \circ F_E^{-1} \ \ \forall E \in \mathcal{T}_h.$$

We will also use $Q^0 : L^2(\Omega, \mathbb{R}^d) \to V_h$, which is the above operator applied component-wise. It follows from (3.5) that

$$\begin{aligned} &\forall\, \phi \in L^2(\Omega, \mathbb{R}^d), \quad (Q^0\phi - \phi, \operatorname{div} \tau) = 0, \quad \forall\, \tau \in \mathbb{X}_h, \\ &\forall\, \phi \in L^2(\Omega), \quad (Q^0\phi - \phi, \operatorname{div} \zeta) = 0, \quad \forall\, \zeta \in Z_h. \end{aligned} \tag{6.3}$$

Let $Q^1 : L^2(\Omega, \mathbb{N}) \to \mathbb{Q}_h$ be the L^2-projection operator satisfying for any $\phi \in L^2(\Omega, \mathbb{N})$,

$$(Q^1\phi - \phi, \xi) = 0, \quad \forall \xi \in \mathbb{Q}_h. \tag{6.4}$$

Let $\Pi : \mathbb{X} \cap H^1(\Omega, \mathbb{M}) \to \mathbb{X}_h$ be the canonical mixed projection operator acting on tensor valued functions. We will also use the same notation for the projection operator acting on vector valued functions, $\Pi : Z \cap H^1(\Omega, \mathbb{R}^d) \to Z_h$. It is shown in [11,12] and [49] that Π satisfies

$$\begin{aligned} &\forall \psi \in H^1(\Omega, \mathbb{M}), \quad (\operatorname{div}(\Pi\psi - \psi), v) = 0, \qquad \forall v \in V_h, \\ &\forall \psi \in H^1(\Omega, \mathbb{R}^d), \quad (\operatorname{div}(\Pi\psi - \psi), w) = 0, \qquad \forall w \in W_h. \end{aligned} \tag{6.5}$$

We will also make use of the mixed projection operator onto the lowest order Raviart–Thomas space $\mathcal{RT}_0$ [11,32,42]. This additional construction is needed only for the error analysis on quadrilaterals, although for uniformity in the forthcoming proofs we will treat the simplicial case in the same fashion. We denote the $\mathcal{RT}_0$-based spaces by $\mathbb{X}_h^0$ and Z_h^0 for tensors and vectors, respectively, where the former is obtained from d copies of the latter. The degrees of freedom of $\mathbb{X}_h^0$ or Z_h^0 are constant values of the normal stress or velocity on all edges (faces). The $\mathcal{RT}_0$ mixed projection operator, denoted by Π^0, has properties similar to the $\mathcal{BDM}_1$ projection operator Π. It also satisfies

$$\begin{aligned} &\operatorname{div}\Pi^0\tau = \operatorname{div}\tau \quad \text{and} \quad \|\Pi^0\tau\| \le C\|\tau\| \quad \forall \tau \in \mathbb{X}_h, \\ &\operatorname{div}\Pi^0\zeta = \operatorname{div}\zeta \quad \text{and} \quad \|\Pi^0\zeta\| \le C\|\zeta\| \quad \forall \zeta \in Z_h. \end{aligned} \tag{6.6}$$

The following lemma summarizes well-known continuity and approximation properties of the projection operators, where $\mathbb{H} \in \{\mathbb{M}, \mathbb{R}^d\}$.

Lemma 6.1. *There exists a constant $C > 0$ such that*

$$\|\phi - Q^0\phi\| \le C\|\phi\|_r h^r, \qquad \forall \phi \in H^r(\Omega), \qquad 0 \le r \le 1, \tag{6.7}$$

$$\|\phi - Q^1\phi\| \le C\|\phi\|_r h^r, \qquad \forall \phi \in H^r(\Omega, \mathbb{N}), \qquad 0 \le r \le 1, \tag{6.8}$$

$$\|\psi - \Pi\psi\| \le C\|\psi\|_r h^r, \qquad \forall \psi \in H^r(\Omega, \mathbb{H}), \qquad 1 \le r \le 2, \tag{6.9}$$

$$\|\psi - \Pi^0\psi\| \le C\|\psi\|_1 h, \qquad \forall \psi \in H^1(\Omega, \mathbb{H}), \tag{6.10}$$

$$\|\operatorname{div}(\psi - \Pi\psi)\| + \|\operatorname{div}(\psi - \Pi^0\psi)\| \le C\|\operatorname{div}\psi\|_r h^r, \qquad \forall \psi \in H^{r+1}(\Omega, \mathbb{H}), \qquad 0 \le r \le 1. \tag{6.11}$$

In addition, for all elements $E \in \mathcal{T}_h$, there exists a constant $C > 0$, such that

$$\|Q^0\phi\|_E \le C\|\phi\|_E, \qquad \forall \phi \in L^2(E), \tag{6.12}$$

$$\|Q^1\phi\|_{1,E} \le C\|\phi\|_{1,E}, \qquad \forall \phi \in H^1(E, \mathbb{N}), \tag{6.13}$$

$$\|\Pi\psi\|_{1,E} \le C\|\psi\|_{1,E}, \qquad \forall \psi \in H^1(E, \mathbb{H}). \tag{6.14}$$

Proof. The proof of bounds for the L^2-projections (6.7)–(6.8) can be found in [14]; and bounds (6.9)–(6.11) can be found in [11,43] for affine elements and [6,49] for h^2-parallelograms. Finally, (6.12) is the stability of the L^2-projection and the proof of (6.13)–(6.14) was presented in [52]. □

The following result is needed in the error analysis.

Lemma 6.2. *For any $\hat{\tau} \in \hat{\mathbb{X}}(\hat{E})$ and $\hat{\zeta} \in \hat{Z}(\hat{E})$,*

$$\left(\hat{\tau} - \hat{\Pi}^0\hat{\tau}, \hat{\tau}_0\right)_{\hat{\mathcal{Q}}, \hat{E}} = 0 \quad \textit{for all constant tensors } \hat{\tau}_0, \tag{6.15}$$

$$\left(\hat{\zeta} - \hat{\Pi}^0\hat{\zeta}, \hat{\zeta}_0\right)_{\hat{\mathcal{Q}}, \hat{E}} = 0 \quad \textit{for all constant vectors } \hat{\zeta}_0. \tag{6.16}$$

Proof. The property (6.16) was shown in [52, Lemma 2.2] on the reference square. The proof on the reference simplex follows in a similar way. The property (6.15) follows from (6.16). □

For $\phi, \psi \in \mathbb{X}_h, \mathbb{Q}_h, Z_h, W_h$, denote the quadrature error by

$$\forall E \in \mathcal{T}_h, \quad \theta_E(L\phi, \psi) := (L\phi, \psi)_E - (L\phi, \psi)_{Q,E}, \quad \theta(L\phi, \psi) := (L\phi, \psi) - (L\phi, \psi)_Q. \tag{6.17}$$

The next result summarizes the quadrature error bounds.

Lemma 6.3. *For all $E \in \mathcal{T}_h$, if $K^{-1}|_E \in W^{1,\infty}(E)$ and $A|_E \in W^{1,\infty}(E)$, then there is a constant $C > 0$ independent of h such that*

$$\left|\theta_E\left(K^{-1}\zeta, \rho\right)\right| \leq Ch\|K^{-1}\|_{1,\infty,E}\|\zeta\|_{1,E}\|\rho\|_E, \qquad \forall \zeta \in Z_h,\ \rho \in Z_h^0, \tag{6.18}$$

$$|\theta_E(A\tau, \chi)| \leq Ch\|A\|_{1,\infty,E}\|\tau\|_{1,E}\|\chi\|_E, \qquad \forall \tau \in \mathbb{X}_h,\ \chi \in \mathbb{X}_h^0, \tag{6.19}$$

$$|\theta_E(A\tau, wI)| \leq Ch\|A\|_{1,\infty,E}\|\tau\|_{1,E}\|w\|_E, \qquad \forall \tau \in \mathbb{X}_h,\ w \in W_h, \tag{6.20}$$

$$|\theta_E(AwI, rI)| \leq Ch\|A\|_{1,\infty,E}\|w\|_E\|r\|_E, \qquad \forall w, r \in W_h, \tag{6.21}$$

$$|\theta_E(\tau, \xi)| \leq Ch\|\tau\|_{1,E}\|\xi\|_E, \qquad \forall \tau \in \mathbb{X}_h, \xi \in \mathbb{Q}_h, \tag{6.22}$$

$$|\theta_E(\tau, \xi)| \leq Ch\|\tau\|_E\|\xi\|_{1,E}, \qquad \forall \tau \in \mathbb{X}_h^0, \xi \in \mathbb{Q}_h, \tag{6.23}$$

$$\left|\left(K^{-1}\rho, \zeta - \Pi^0\zeta\right)_{Q,E}\right| \leq Ch\|K^{-1}\|_{1,\infty,E}\|\rho\|_{1,E}\|\zeta\|_E, \qquad \forall \rho, \zeta \in Z_h, \tag{6.24}$$

$$\left|\left(A(\chi + wI), \tau - \Pi^0\tau\right)_{Q,E}\right| \leq Ch\|A\|_{1,\infty,E}(\|\chi\|_{1,E} + \|w\|_E)\|\tau\|_E, \qquad \forall \chi, \tau \in \mathbb{X}_h, w \in W_h, \tag{6.25}$$

$$\left|\left(\xi, \tau - \Pi^0\tau\right)_{Q,E}\right| \leq Ch\|\xi\|_{1,E}\|\tau\|_E, \qquad \forall \xi \in \mathbb{Q}_h, \tau \in \mathbb{X}_h. \tag{6.26}$$

Proof. The estimates (6.18) and (6.24) can be found in [52]. We note that (6.24) was stated only on quadrilaterals in [52], but it also holds on simplices, since it follows from mapping to the reference element and (6.16). Bounds (6.19) and (6.22)–(6.23) were proven in [3] on simplices and in [2] on quadrilaterals. The proofs of bounds (6.20)–(6.21) for the two element types are similar to the respective proofs of (6.19). Bounds (6.25) and (6.26) were shown in [2] on quadrilaterals. Their proof on simplices is similar, using (6.15). □

Remark 6.1. We note that, since the $\mathcal{BDM}_1$ space on quadrilaterals involves quadratic terms, the quadrature bounds (6.18), (6.19), and (6.23) require restricting one of the test functions to the $\mathcal{RT}_0$ space, which also leads to the additional error terms in (6.24)–(6.26). This restriction is not necessary on simplices, where $\mathcal{BDM}_1$ is the space of linear polynomials. In order to present a unified convergence proof for simplices and quadrilaterals, we make the restriction to $\mathcal{RT}_0$ on simplices as well. A simplified proof without this restriction on simplices is also possible, following the approaches in [52] and [3].

The above bounds are stated on an element $E \in \mathcal{T}_h$. In the convergence proof they will be used by summing over all elements. We will assume that $\|K^{-1}\|_{1,\infty,E}$ and $\|A\|_{1,\infty,E}$ are uniformly bounded independently of h and will denote this space by $W^{1,\infty}_{\mathcal{T}_h}$.

6.2. Main convergence result

Theorem 6.1. *If $A \in W^{1,\infty}_{\mathcal{T}_h}$, $K^{-1} \in W^{1,\infty}_{\mathcal{T}_h}$, and the solution of (2.8)–(2.12) is sufficiently smooth, then there exists a positive constant C independent of h and c_0, such that the solution of (3.13)–(3.17) satisfies*

$$\begin{aligned}
&\|\sigma - \sigma_h\|_{L^\infty(0,T;H(\mathrm{div};\Omega))} + \|u - u_h\|_{L^\infty(0,T;L^2(\Omega))} + \|\gamma - \gamma_h\|_{L^\infty(0,T;L^2(\Omega))} + \|z - z_h\|_{L^\infty(0,T;L^2(\Omega))} \\
&\quad + \|p - p_h\|_{L^\infty(0,T;L^2(\Omega))} + \|\sigma - \sigma_h\|_{L^2(0,T;H(\mathrm{div};\Omega))} + \|u - u_h\|_{L^2(0,T;L^2(\Omega))} \\
&\quad + \|\gamma - \gamma_h\|_{L^2(0,T;L^2(\Omega))} + \|z - z_h\|_{L^2(0,T;H(\mathrm{div};\Omega))} + \|p - p_h\|_{L^2(0,T;L^2(\Omega))} \\
&\leq Ch\Big(\|\sigma\|_{H^1(0,T;H^1(\Omega))} + \|\mathrm{div}\,\sigma\|_{L^\infty(0,T;H^1(\Omega))} + \|\mathrm{div}\,\sigma\|_{L^2(0,T;H^1(\Omega))} \\
&\quad + \|u\|_{L^2(0,T;H^1(\Omega))} + \|u\|_{L^\infty(0,T;H^1(\Omega))} + \|\gamma\|_{H^1(0,T;H^1(\Omega))} \\
&\quad + \|z\|_{H^1(0,T;H^1(\Omega))} + \|\mathrm{div}\,z\|_{L^2(0,T;H^1(\Omega))} + \|p\|_{H^1(0,T;H^1(\Omega))}\Big).
\end{aligned} \tag{6.27}$$

Proof. The derivation of the error bounds follows the structure of the stability analysis. It involves special manipulation of the error system, combined with estimation of the approximation errors and the quadrature errors. We form the error system by subtracting the discrete problem (3.13)–(3.17) from the continuous one (2.8)–(2.12):

$$(A(\sigma + \alpha pI), \tau) - (A(\sigma_h + \alpha p_h I), \tau)_Q + (u - u_h, \mathrm{div}\,\tau) + (\gamma, \tau) - (\gamma_h, \tau)_Q = 0, \qquad \forall \tau \in \mathbb{X}_h, \tag{6.28}$$

$$(\operatorname{div}(\sigma - \sigma_h), v) = 0, \qquad \forall v \in V_h, \tag{6.29}$$

$$(\sigma, \xi) - (\sigma_h, \xi)_Q = 0, \qquad \forall \xi \in \mathbb{Q}_h, \tag{6.30}$$

$$\left(K^{-1}z, \zeta\right) - \left(K^{-1}z_h, \zeta\right)_Q - (p - p_h, \operatorname{div}\zeta) = 0, \qquad \forall \zeta \in Z_h, \tag{6.31}$$

$$\begin{aligned}(c_0\partial_t(p - p_h), w) + \alpha\,(\partial_t A(\sigma + \alpha p I), wI) - \alpha\,(\partial_t A(\sigma_h + \alpha p_h I), wI)_Q \\ + (\operatorname{div}(z - z_h), w) = 0, \qquad \forall w \in W_h.\end{aligned} \tag{6.32}$$

We split the errors into approximation and discrete errors as follows:

$$\begin{aligned}\sigma - \sigma_h &= (\sigma - \Pi\sigma) + (\Pi\sigma - \sigma_h) := \psi_\sigma + \phi_\sigma,\\ u - u_h &= (u - Q^0 u) + (Q^0 u - u_h) := \psi_u + \phi_u,\\ \gamma - \gamma_h &= (\gamma - Q^1\gamma) + (Q^1\gamma - \gamma_h) := \psi_\gamma + \phi_\gamma,\\ z - z_h &= (z - \Pi z) + (\Pi z - z_h) := \psi_z + \phi_z,\\ p - p_h &= (p - Q^0 p) + (Q^0 p - p_h) := \psi_p + \phi_p.\end{aligned}$$

We first manipulate the error system (6.28)–(6.32) to obtain error terms that can be bounded using either the orthogonality and approximation properties of the projection operators, (6.3)–(6.5) and (6.7)–(6.11), or the estimates for the quadrature error terms, (6.18)–(6.26). We rewrite the first equation (6.28) in the following way:

$$\begin{aligned}&\left(A(\phi_\sigma + \alpha\phi_p I), \tau\right)_Q + (\phi_u, \operatorname{div}\tau) + \left(\phi_\gamma, \tau\right)_Q\\ &\quad = -\left(A(\sigma + \alpha p I), \tau\right) + \left(A(\Pi\sigma + \alpha Q^0 p I), \tau\right)_Q + (\psi_u, \operatorname{div}\tau) + \left(Q^1\gamma, \tau\right)_Q - (\gamma, \tau).\end{aligned}$$

It follows from (6.3) that $(\psi_u, \operatorname{div}\tau) = 0$. With the goal to use a test function $\Pi^0\tau$, which is needed to bound the quadrature error, we manipulate the rest of the terms as follows:

$$\begin{aligned}&\left(A(\phi_\sigma + \alpha\phi_p I), \tau\right)_Q + (\phi_u, \operatorname{div}\tau) + \left(\phi_\gamma, \tau\right)_Q\\ &\quad = -\left(A(\sigma + \alpha p I), \tau - \Pi^0\tau\right) - \left(A(\psi_\sigma + \alpha\psi_p I), \Pi^0\tau\right) - \left(A(\Pi\sigma + \alpha Q^0 p I), \Pi^0\tau\right)\\ &\qquad + \left(A(\Pi\sigma + \alpha Q^0 p I), \Pi^0\tau\right)_Q + \left(A(\Pi\sigma + \alpha Q^0 p I), \tau - \Pi^0\tau\right)_Q\\ &\qquad - \left(\gamma, \tau - \Pi^0\tau\right) - \left(\psi_\gamma, \Pi^0\tau\right) - \left(Q^1\gamma, \Pi^0\tau\right) + \left(Q^1\gamma, \Pi^0\tau\right)_Q + \left(Q^1\gamma, \tau - \Pi^0\tau\right)_Q.\end{aligned} \tag{6.33}$$

Taking $\tau - \Pi^0\tau$ as a test function in (2.8) and using (6.6), we obtain

$$\left(A(\sigma + \alpha p I), \tau - \Pi^0\tau\right) + \left(\gamma, \tau - \Pi^0\tau\right) = 0. \tag{6.34}$$

Combining (6.33)–(6.34) and using the quadrature error notation, we get

$$\begin{aligned}&\left(A(\phi_\sigma + \alpha\phi_p I), \tau\right)_Q + (\phi_u, \operatorname{div}\tau) + \left(\phi_\gamma, \tau\right)_Q\\ &\quad = -\left(A(\psi_\sigma + \alpha\psi_p I), \Pi^0\tau\right) - \left(\psi_\gamma, \Pi^0\tau\right) - \theta\left(A(\Pi\sigma + \alpha Q^0 p I), \Pi^0\tau\right) - \theta\left(Q^1\gamma, \Pi^0\tau\right)\\ &\qquad + \left(A(\Pi\sigma + \alpha Q^0 p I), \tau - \Pi^0\tau\right)_Q + \left(Q^1\gamma, \tau - \Pi^0\tau\right)_Q.\end{aligned} \tag{6.35}$$

We proceed with the manipulation of the rest of the equations in the error system (6.28)–(6.32). Using (6.5) and taking $v = J_E \operatorname{div}\phi_\sigma$ on each $E \in \mathcal{T}_h$, the second error Eq. (6.29) implies

$$\operatorname{div}\phi_\sigma = 0. \tag{6.36}$$

We rewrite the third error Eq. (6.30) as

$$(\psi_\sigma, \xi) + \theta\,(\Pi\sigma, \xi) + (\phi_\sigma, \xi)_Q = 0. \tag{6.37}$$

We rewrite the Darcy's law error Eq. (6.31) in a way similar to (6.33)–(6.35):

$$\begin{aligned}\left(K^{-1}\phi_z, \zeta\right)_Q - \left(\phi_p, \operatorname{div}\zeta\right) &= -\left(K^{-1}z, \zeta - \Pi^0\zeta\right) - \left(K^{-1}(z - \Pi z), \Pi^0\zeta\right) - \left(K^{-1}\Pi z, \Pi^0\zeta\right)\\ &\quad + \left(K^{-1}\Pi z, \Pi^0\zeta\right)_Q + \left(K^{-1}\Pi z, \zeta - \Pi^0\zeta\right)_Q + \left(\psi_p, \operatorname{div}\zeta\right).\end{aligned}$$

Using (6.3), we have that $\left(\psi_p, \operatorname{div}\zeta\right) = 0$. Also, testing (2.11) with $\zeta - \Pi^0\zeta$ yields $\left(K^{-1}z, \zeta - \Pi^0\zeta\right) = 0$, hence, we have

$$\left(K^{-1}\phi_z, \zeta\right)_Q - \left(\phi_p, \operatorname{div}\zeta\right) = -\left(K^{-1}\psi_z, \Pi^0\zeta\right) - \theta\left(K^{-1}\Pi z, \Pi^0\zeta\right) + \left(K^{-1}\Pi z, \zeta - \Pi^0\zeta\right)_Q. \tag{6.38}$$

Finally, using (6.5), we rewrite the last equation in the error system, (6.32), as follows,

$$\begin{aligned}&\left(c_0\partial_t\phi_p, w\right) + \alpha\left(\partial_t A(\phi_\sigma + \alpha\phi_p I), wI\right)_Q + (\operatorname{div}\phi_z, w)\\ &\qquad = -\left(c_0\partial_t\psi_p, w\right) - \alpha\left(\partial_t A(\psi_\sigma + \alpha\psi_p I), wI\right) - \alpha\theta\left(\partial_t A(\Pi\sigma + \alpha Q^0 pI), wI\right).\end{aligned} \tag{6.39}$$

We next combine the equations and make an appropriate choice of the test functions. In particular, we differentiate (6.35) in time, set $\tau = \phi_\sigma$, $\xi = \partial_t\phi_\gamma$, $\zeta = \phi_z$, $w = \phi_p$, and combine (6.35)–(6.39):

$$\begin{aligned}&\frac{1}{2}\partial_t\left(\|A^{1/2}(\phi_\sigma + \alpha\phi_p I)\|_Q^2 + \|c_0^{1/2}\phi_p\|^2\right) + \|K^{-1/2}\phi_z\|_Q^2\\ &\quad = -\left(c_0\partial_t\psi_p, \phi_p\right) - \left(\partial_t A(\psi_\sigma + \alpha\psi_p I), \Pi^0\phi_\sigma + \alpha\phi_p I\right) - \left(\partial_t\psi_\gamma, \Pi^0\phi_\sigma\right) - \left(K^{-1}\psi_z, \Pi^0\phi_z\right) + \left(\psi_\sigma, \partial_t\phi_\gamma\right)\\ &\qquad - \theta\left(\partial_t A(\Pi\sigma + \alpha Q^0 pI), \Pi^0\phi_\sigma + \alpha\phi_p I\right) - \theta\left(\partial_t Q^1\gamma, \Pi^0\phi_\sigma\right) - \theta\left(K^{-1}\Pi z, \Pi^0\phi_z\right) + \theta\left(\Pi\sigma, \partial_t\phi_\gamma\right)\\ &\qquad + \left(\partial_t A(\Pi\sigma + \alpha Q^0 pI), \phi_\sigma - \Pi^0\phi_\sigma\right)_Q + \left(\partial_t Q^1\gamma, \phi_\sigma - \Pi^0\phi_\sigma\right)_Q + \left(K^{-1}\Pi z, \phi_z - \Pi^0\phi_z\right)_Q,\end{aligned} \tag{6.40}$$

where we have listed first the terms involving approximation error, followed by quadrature error terms, and the three extra terms arising from the use of operator Π^0. We note that there are two terms involving $\partial_t\phi_\gamma$, which will be handled by integration by parts after time integration. We proceed by deriving bounds for the rest of the terms appearing on the right-hand side. For the approximation error terms, using (6.6) and (6.7)–(6.9), we have

$$\begin{aligned}&\left|\left(c_0\partial_t\psi_p, \phi_p\right) + \left(\partial_t A(\psi_\sigma + \alpha\psi_p I), \Pi^0\phi_\sigma + \alpha\phi_p I\right) + \left(\partial_t\psi_\gamma, \Pi^0\phi_\sigma\right) + \left(K^{-1}\psi_z, \Pi^0\phi_z\right)\right|\\ &\qquad \le Ch^2(\|\partial_t\sigma\|_1^2 + \|\partial_t p\|_1^2 + \|\partial_t\gamma\|_1^2 + \|z\|_1^2) + \epsilon_1(\|\phi_\sigma\|^2 + \|\phi_p\|^2 + \|\phi_z\|^2).\end{aligned} \tag{6.41}$$

For the quadrature error terms, applying (6.18)–(6.14) and (6.21)–(6.12) results in

$$\begin{aligned}&\left|\theta\left(\partial_t A(\Pi\sigma + \alpha Q^0 pI), \Pi^0\phi_\sigma + \alpha\phi_p I\right) + \theta\left(\partial_t Q^1\gamma, \Pi^0\phi_\sigma\right) + \theta\left(K^{-1}\Pi z, \Pi^0\phi_z\right)\right|\\ &\qquad \le Ch^2(\|\partial_t\sigma\|_1^2 + \|\partial_t p\|_1^2 + \|\partial_t\gamma\|_1^2 + \|z\|_1^2) + \epsilon_1(\|\phi_\sigma\|^2 + \|\phi_p\|^2 + \|\phi_z\|^2).\end{aligned} \tag{6.42}$$

For the last three terms in (6.40), due to (6.24)–(6.14) and (6.26)–(6.13), we obtain

$$\begin{aligned}&\left|\left(\partial_t A(\Pi\sigma + \alpha Q^0 pI), \phi_\sigma - \Pi^0\phi_\sigma\right)_Q + \left(\partial_t Q^1\gamma, \phi_\sigma - \Pi^0\phi_\sigma\right)_Q + \left(K^{-1}\Pi z, \phi_z - \Pi^0\phi_z\right)_Q\right|\\ &\qquad \le Ch^2(\|\partial_t\sigma\|_1^2 + \|\partial_t p\|_1^2 + \|\partial_t\gamma\|_1^2 + \|z\|_1^2) + \epsilon_1(\|\phi_\sigma\|^2 + \|\phi_z\|^2).\end{aligned} \tag{6.43}$$

Next, we combine (6.40)–(6.43) and integrate in time from 0 to an arbitrary $t \in (0, T]$:

$$\begin{aligned}&\|A^{1/2}(\phi_\sigma + \alpha\phi_p I)(t)\|_Q^2 + \|c_0^{1/2}\phi_p(t)\|^2 + \int_0^t \|K^{-1/2}\phi_z\|_Q^2\, ds\\ &\quad \le \int_0^t \left(\left(\psi_\sigma, \partial_t\phi_\gamma\right) + \theta\left(\Pi\sigma, \partial_t\phi_\gamma\right)\right) ds + \epsilon_1\int_0^t (\|\phi_\sigma\|^2 + \|\phi_p\|^2 + \|\phi_z\|^2)\, ds\\ &\qquad + Ch^2\int_0^t (\|\partial_t\sigma\|_1^2 + \|\partial_t p\|_1^2 + \|\partial_t\gamma\|_1^2 + \|z\|_1^2)\, ds + \|A^{1/2}(\phi_\sigma + \alpha\phi_p I)(0)\|_Q^2 + \|c_0^{1/2}\phi_p(0)\|^2.\end{aligned} \tag{6.44}$$

For the first two terms on the right-hand side we use integration by parts:

$$\begin{aligned}&\int_0^t \left(\left(\psi_\sigma, \partial_t\phi_\gamma\right) + \theta\left(\Pi\sigma, \partial_t\phi_\gamma\right)\right) ds\\ &\quad = -\int_0^t \left(\left(\partial_t\psi_\sigma, \phi_\gamma\right) + \theta\left(\partial_t\Pi\sigma, \phi_\gamma\right)\right) ds + \left(\psi_\sigma, \phi_\gamma\right)(t) + \theta\left(\Pi\sigma, \phi_\gamma\right)(t) - \left(\psi_\sigma, \phi_\gamma\right)(0) - \theta\left(\Pi\sigma, \phi_\gamma\right)(0)\\ &\quad \le \epsilon_1\left(\|\phi_\gamma(t)\|^2 + \int_0^t \|\phi_\gamma\|^2 ds\right) + C\|\phi_\gamma(0)\|^2 + Ch^2\left(\|\sigma(t)\|_1^2 + \|\sigma(0)\|_1^2 + \int_0^t \|\partial_t\sigma\|_1^2\, ds\right).\end{aligned} \tag{6.45}$$

where we used (6.9), (6.22), and (6.14) in the last step. We proceed with bounding the terms involving $\|\phi_\sigma\|$, $\|\phi_p\|$, $\|\phi_z\|$, and $\|\phi_\gamma\|$ that appear on the right-hand sides of (6.44) and (6.45). Using the elasticity inf–sup condition

(4.2) together with (6.28), we get

$$\begin{aligned}\|\phi_u\| + \|\phi_\gamma\| \leq & C \sup_{0\neq\tau\in\mathbb{X}_h} \frac{(\phi_u, \operatorname{div}\tau) + \left(\phi_\gamma, \tau\right)_Q}{\|\tau\|_{\operatorname{div}}} \\ = & C \sup_{0\neq\tau\in\mathbb{X}_h} \frac{(A(\sigma_h + \alpha p_h I), \tau)_Q - (A(\sigma + \alpha p I), \tau) + \left(Q^1\gamma, \tau\right)_Q - (\gamma, \tau)}{\|\tau\|_{\operatorname{div}}}. \end{aligned} \tag{6.46}$$

Using manipulations as in (6.33)–(6.35), along with the bounds (6.7)–(6.9), (6.19), (6.22) and (6.25)–(6.26), we have

$$\begin{aligned}&(A(\sigma_h + \alpha p_h I), \tau)_Q - (A(\sigma + \alpha p I), \tau) + \left(Q^1\gamma, \tau\right) - (\gamma, \tau)_Q \\ &\quad = -\left(A(\phi_\sigma + \alpha\phi_p I), \tau\right)_Q - \left(A(\psi_\sigma + \alpha\psi_p I), \Pi^0\tau\right) - \left(A(\Pi\sigma + \alpha Q^0 p I), \tau - \Pi^0\tau\right)_Q \\ &\qquad + \theta\left(A(\Pi\sigma + \alpha Q^0 p I), \Pi^0\tau\right)_Q + \left(Q^1\gamma, \tau - \Pi^0\tau\right)_Q - \theta\left(Q^1\gamma, \Pi^0\tau\right) - \left(\psi_\gamma, \Pi^0\tau\right) \\ &\quad \leq C\left(h(\|\sigma\|_1 + \|p\|_1 + \|\gamma\|_1) + \|A^{1/2}(\phi_\sigma + \alpha\phi_p I)\|\right)\|\tau\|. \end{aligned} \tag{6.47}$$

Combining (6.46) and (6.47), we obtain

$$\|\phi_u\| + \|\phi_\gamma\| \leq Ch(\|\sigma\|_1 + \|p\|_1 + \|\gamma\|_1) + C\|A^{1/2}(\phi_\sigma + \alpha\phi_p I)\|, \tag{6.48}$$

as well as

$$\int_0^t \left(\|\phi_u\|^2 + \|\phi_\gamma\|^2\right) ds \leq Ch^2 \int_0^t \left(\|\sigma\|_1^2 + \|p\|_1^2 + \|\gamma\|_1^2\right) ds + C\int_0^t \left(\|\phi_\sigma\|^2 + \|\phi_p\|^2\right) ds. \tag{6.49}$$

For $\|\phi_p\|$, using the fact that $Z_h^0 \times W_h$ is a stable Darcy pair, (6.9), (6.18) and (6.31), we obtain

$$\begin{aligned}\|\phi_p\| \leq & C \sup_{0\neq\zeta\in Z_h^0} \frac{(\operatorname{div}\zeta, \phi_p)}{\|\zeta\|_{\operatorname{div}}} = C \sup_{0\neq\zeta\in Z_h^0} \frac{\left(K^{-1}z, \zeta\right) - \left(K^{-1}z_h, \zeta\right)_Q}{\|\zeta\|_{\operatorname{div}}} \\ = & C \sup_{0\neq\zeta\in Z_h^0} \frac{\left(K^{-1}\phi_z, \zeta\right)_Q - \left(K^{-1}\psi_z, \zeta\right) + \theta\left(K^{-1}\Pi z, \zeta\right)}{\|\zeta\|_{\operatorname{div}}} \leq C(h\|z\|_1 + \|K^{-1/2}\phi_z\|), \end{aligned} \tag{6.50}$$

implying

$$\int_0^t \|\phi_p\|^2 ds \leq C\int_0^t \left(h^2\|z\|_1^2 + \|K^{-1/2}\phi_z\|^2\right) ds. \tag{6.51}$$

Finally, to obtain a bound on $\int_0^t \|\phi_\sigma\|^2 ds$, which appears on the right hand side in (6.49), we choose $\tau = \phi_\sigma$ in (6.35) and $\xi = \phi_\gamma$ in (6.37) and combine them, using also (6.36), to obtain

$$\begin{aligned}\|A^{1/2}\phi_\sigma\|_Q^2 = & -\alpha\left(A\phi_p I, \phi_\sigma\right)_Q - \left(A(\psi_\sigma + \alpha\psi_p I), \Pi^0\phi_\sigma\right) - \left(\psi_\gamma, \Pi^0\phi_\sigma\right) \\ & - \theta\left(A(\Pi\sigma + \alpha Q^0 p I), \Pi^0\phi_\sigma\right) - \theta\left(Q^1\gamma, \Pi^0\phi_\sigma\right) + \left(A(\Pi\sigma + \alpha Q^0 p I), \phi_\sigma - \Pi^0\phi_\sigma\right)_Q \\ & + \left(Q^1\gamma, \phi_\sigma - \Pi^0\phi_\sigma\right)_Q + (\psi_\sigma, \phi_\gamma) + \theta(\Pi\sigma, \phi_\gamma) \\ \leq & Ch^2(\|\sigma\|_1^2 + \|p\|_1^2 + \|\gamma\|_1^2) + C\|\phi_p\|^2 + \epsilon_2(\|\phi_\gamma\|^2 + \|\phi_\sigma\|^2), \end{aligned}$$

where in the last step we used (6.6), (6.7)–(6.9), (6.19), (6.22), (6.23), (6.25), and (6.26). Thus, we have

$$\int_0^t \|\phi_\sigma\|^2 ds \leq Ch^2 \int_0^t (\|\sigma\|_1^2 + \|p\|_1^2 + \|\gamma\|_1^2) ds + C\int_0^t \|\phi_p\|^2 ds + \epsilon_2 \int_0^t \|\phi_\gamma\|^2 ds. \tag{6.52}$$

Combining (6.36), (6.44)–(6.52) and choosing ϵ_2 small enough, then ϵ_1 small enough, gives the estimate

$$\begin{aligned}&\|A^{1/2}(\phi_\sigma + \alpha\phi_p I)(t)\|^2 + \|\phi_u(t)\|^2 + \|\phi_\gamma(t)\|^2 + \|c_0^{1/2}\phi_p(t)\|^2 + \|\operatorname{div}\phi_\sigma\|^2 \\ &\qquad + \int_0^t \left(\|\phi_\sigma\|^2 + \|\phi_u\|^2 + \|\phi_\gamma\|^2 + \|K^{-1/2}\phi_z\|^2 + \|\phi_p\|^2 + \|\operatorname{div}\phi_\sigma\|^2\right) ds \\ &\quad \leq C\Big(h^2 \int_0^t \left(\|\partial_t\sigma\|_1^2 + \|\partial_t p\|_1^2 + \|\partial_t\gamma\|_1^2 + \|\sigma\|_1^2 + \|p\|_1^2 + \|\gamma\|_1^2 + \|z\|_1^2\right) ds \end{aligned}$$

$$+ h^2 \left(\|\sigma(t)\|_1^2 + \|p(t)\|_1^2 + \|\gamma(t)\|_1^2 + \|\sigma(0)\|_1^2 \right)$$
$$+ \|\phi_\sigma(0)\|^2 + \|\phi_p(0)\|^2 + \|\phi_\gamma(0)\|^2 \Big). \tag{6.53}$$

Estimate for $\operatorname{div}\phi_z$. We note that (6.53) is a self-contained error estimate. Similarly to the stability argument, we proceed with bounding $\|\operatorname{div}\phi_z\|$, obtaining also bounds on $\|K^{-1/2}\phi_z(t)\|$ and $\|\phi_p(t)\|$ for all t. We choose $w = J_E \operatorname{div}\phi_z$ on each $E \in \mathcal{T}_h$ in (6.39), which yields

$$\|J_E^{1/2}\operatorname{div}\phi_z\|^2 = -\left(c_0\partial_t\phi_p, J_E\operatorname{div}\phi_z\right) - \left(c_0\partial_t\psi_p, J_E\operatorname{div}\phi_z\right) - \alpha\left(\partial_t A(\phi_\sigma + \alpha\phi_p I), J_E(\operatorname{div}\phi_z)I\right)_Q$$
$$- \alpha\left(\partial_t A(\psi_\sigma + \alpha\psi_p I), J_E(\operatorname{div}\phi_z)I\right) - \alpha\theta\left(\partial_t A(\Pi\sigma + \alpha Q^0 pI), J_E(\operatorname{div}\phi_z)I\right).$$

Using (6.7), (6.9) and (6.19)–(6.22), we obtain

$$\|\operatorname{div}\phi_z\| \le C\left(\|c_0^{1/2}\partial_t\phi_p\| + \|\partial_t A^{1/2}(\phi_\sigma + \alpha\phi_p I)\| + h(\|\partial_t p\|_1 + \|\partial_t\sigma\|_1)\right). \tag{6.54}$$

It remains to bound the first two terms on the right-hand side of (6.54). Similarly to the stability argument, cf. (5.11), we differentiate (6.35)–(6.38) in time, set $\tau = \partial_t\phi_\sigma$, $\xi = \partial_t\phi_\gamma$, $\zeta = \phi_z$, $w = \partial_t\phi_p$, and combine (6.35)–(6.39), resulting in a time-differentiated version of (6.40):

$$\frac{1}{2}\partial_t\|K^{-1/2}\phi_z\|_Q^2 + \|\partial_t A^{1/2}(\phi_\sigma + \alpha\phi_p I)\|_Q^2 + \|c_0^{1/2}\partial_t\phi_p\|^2$$
$$= -\left(c_0\partial_t\psi_p, \partial_t\phi_p\right) - \left(\partial_t A(\psi_\sigma + \alpha\psi_p I), \partial_t(\Pi^0\phi_\sigma + \alpha\phi_p I)\right) - \left(\partial_t\psi_\gamma, \partial_t\Pi^0\phi_\sigma\right) - \left(\partial_t K^{-1}\psi_z, \Pi^0\phi_z\right)$$
$$+ \left(\partial_t\psi_\sigma, \partial_t\phi_\gamma\right) - \theta\left(\partial_t A(\Pi\sigma + \alpha Q^0 pI), \partial_t(\Pi^0\phi_\sigma + \alpha\phi_p I)\right) - \theta\left(\partial_t Q^1\gamma, \partial_t\Pi^0\phi_\sigma\right)$$
$$- \theta\left(\partial_t K^{-1}\Pi z, \Pi^0\phi_z\right) + \theta\left(\partial_t\Pi\sigma, \partial_t\phi_\gamma\right) + \left(\partial_t A(\Pi\sigma + \alpha Q^0 pI), \partial_t(\phi_\sigma - \Pi^0\phi_\sigma)\right)_Q$$
$$+ \left(\partial_t Q^1\gamma, \partial_t(\phi_\sigma - \Pi^0\phi_\sigma)\right)_Q + \left(\partial_t K^{-1}\Pi z, \phi_z - \Pi^0\phi_z\right)_Q. \tag{6.55}$$

Before bounding the terms on the right above, we note that we would like the bounds to be in terms of $\|\partial_t A^{1/2}(\phi_\sigma + \alpha\phi_p I)\|$, since we do not have separate control of $\|\partial_t\phi_\sigma\|$ and $\|\partial_t\phi_p\|$. To this end, we first note that the projector Π^0 is defined element by element and let $\Pi_E^0 : H^1(E, \mathbb{M}) \mapsto \mathbb{X}_h^0|_E$ be the local $\mathcal{RT}_0$ projector on an element $E \in \mathcal{T}_h$. Using that for each E, $\alpha\phi_p I|_E \in \mathbb{X}_h^0|_E$, we have that $\Pi_E^0(\alpha\phi_p I) = (\alpha\phi_p I)|_E$. Then, for the second and the sixth term above we have

$$(\Pi^0\phi_\sigma + \alpha\phi_p I)|_E = \Pi_E^0(\phi_\sigma + \alpha\phi_p I).$$

Similarly, for the tenth and the eleventh term we have

$$(\phi_\sigma - \Pi^0\phi_\sigma)|_E = (\phi_\sigma + \alpha\phi_p I)|_E - \Pi_E^0(\phi_\sigma + \alpha\phi_p I).$$

Also, since $\phi_p I$ is a symmetric matrix, for the third and seventh terms we have

$$\left(\partial_t\psi_\gamma, \partial_t\Pi^0\phi_\sigma\right)_E = \left(\partial_t\psi_\gamma, \partial_t\Pi_E^0(\phi_\sigma + \alpha\phi_p I)\right)_E, \quad \theta_E\left(\partial_t Q^1\gamma, \partial_t\Pi^0\phi_\sigma\right) = \theta_E\left(\partial_t Q^1\gamma, \partial_t\Pi_E^0(\phi_\sigma + \alpha\phi_p I)\right).$$

Now, noting that the terms on the right in (6.55) can be expressed as sums over mesh elements, we use the above identities and bound these terms as in (6.41)–(6.43):

$$\left|\left(c_0\partial_t\psi_p, \partial_t\phi_p\right) + \left(\partial_t A(\psi_\sigma + \alpha\psi_p I), \partial_t(\Pi^0\phi_\sigma + \alpha\phi_p I)\right) + \left(\partial_t\psi_\gamma, \partial_t\Pi^0\phi_\sigma\right)\right.$$
$$\left. + \left(\partial_t K^{-1}\psi_z, \Pi^0\phi_z\right) + \left(\partial_t\psi_\sigma, \partial_t\phi_\gamma\right)\right|$$
$$\le Ch^2(\|\partial_t\sigma\|_1^2 + \|\partial_t p\|_1^2 + \|\partial_t\gamma\|_1^2 + \|\partial_t z\|_1^2)$$
$$+ \epsilon(\|c_0^{1/2}\partial_t\phi_p\|^2 + \|\partial_t A^{1/2}(\phi_\sigma + \alpha\phi_p I)\|^2 + \|\partial_t\phi_\gamma\|^2 + \|\phi_z\|^2), \tag{6.56}$$

$$\left|\theta\left(\partial_t A(\Pi\sigma + \alpha Q^0 pI), \partial_t(\Pi^0\phi_\sigma + \alpha\phi_p I)\right) + \theta\left(\partial_t Q^1\gamma, \partial_t\Pi^0\phi_\sigma\right) + \theta\left(\partial_t K^{-1}\Pi z, \Pi^0\phi_z\right) + \theta\left(\partial_t\Pi\sigma, \partial_t\phi_\gamma\right)\right|$$
$$\le Ch^2(\|\partial_t\sigma\|_1^2 + \|\partial_t p\|_1^2 + \|\partial_t\gamma\|_1^2 + \|\partial_t z\|_1^2) + \epsilon(\|\partial_t A^{1/2}(\phi_\sigma + \alpha\phi_p I)\|^2 + \|\partial_t\phi_\gamma\|^2 + \|\phi_z\|^2), \tag{6.57}$$

$$\left|\left(\partial_t A(\Pi\sigma + \alpha Q^0 pI), \partial_t(\phi_\sigma - \Pi^0\phi_\sigma)\right)_Q + \left(\partial_t Q^1\gamma, \partial_t(\phi_\sigma - \Pi^0\phi_\sigma)\right)_Q + \left(\partial_t K^{-1}\Pi z, \phi_z - \Pi^0\phi_z\right)_Q\right|$$
$$\le Ch^2(\|\partial_t\sigma\|_1^2 + \|\partial_t p\|_1^2 + \|\partial_t\gamma\|_1^2 + \|\partial_t z\|_1^2) + \epsilon(\|\partial_t A^{1/2}(\phi_\sigma + \alpha\phi_p I)\|^2 + \|\phi_z\|^2). \tag{6.58}$$

Combining (6.55)–(6.58), taking ϵ small enough, and integrating in time, we get

$$\begin{aligned}
&\|K^{-1/2}\phi_z(t)\|_Q^2 + \int_0^t \left(\|\partial_t A^{1/2}(\phi_\sigma + \alpha\phi_p I)\|_Q^2 + \|c_0^{1/2}\partial_t\phi_p\|^2\right) ds \\
&\quad \le \|K^{-1/2}\phi_z(0)\|_Q^2 + \epsilon \int_0^t \left(\|\partial_t\phi_\gamma\|^2 + \|\phi_z\|^2\right) ds \\
&\quad\quad + Ch^2 \int_0^t \left(\|\partial_t\sigma\|_1^2 + \|\partial_t p\|_1^2 + \|\partial_t\gamma\|_1^2 + \|\partial_t z\|_1^2\right) ds. \qquad (6.59)
\end{aligned}$$

Similarly to (6.48), the elasticity inf–sup condition (4.2), differentiated in time, implies

$$\int_0^t \left(\|\partial_t\phi_u\|^2 + \|\partial_t\phi_\gamma\|^2\right) ds \le Ch^2 \int_0^t \left(\|\partial_t\sigma\|_1^2 + \|\partial_t p\|_1^2 + \|\partial_t\gamma\|_1^2\right) ds + C\int_0^t \|\partial_t A^{1/2}(\phi_\sigma + \alpha\phi_p I)\|^2 ds. \qquad (6.60)$$

Combining (6.59)–(6.60) with (6.50), we conclude that

$$\begin{aligned}
&\|K^{-1/2}\phi_z(t)\|^2 + \|\phi_p(t)\|^2 + \int_0^t \left(\|\partial_t A^{1/2}(\phi_\sigma + \alpha\phi_p I)\|^2 + \|c_0^{1/2}\partial_t\phi_p\|^2\right) ds \\
&\quad \le \epsilon \int_0^t \|\phi_z\|^2 ds + Ch^2\|z(t)\|^2 \\
&\quad\quad + Ch^2 \int_0^t \left(\|\partial_t\sigma\|_1^2 + \|\partial_t p\|_1^2 + \|\partial_t\gamma\|_1^2 + \|\partial_t z\|_1^2\right) ds. \qquad (6.61)
\end{aligned}$$

Therefore, (6.54) and (6.61) give

$$\begin{aligned}
&\|K^{-1/2}\phi_z(t)\|_Q^2 + \|\phi_p(t)\|^2 + \int_0^t \|\operatorname{div}\phi_z\|^2 ds \le \epsilon \int_0^t \|\phi_z\|^2 ds \\
&\quad + Ch^2 \left(\int_0^t (\|\partial_t z\|_1^2 + \|\partial_t\sigma\|_1^2 + \|\partial_t p\|_1^2 + \|\partial_t\gamma\|_1^2) ds + \|z(t)\|_1^2\right). \qquad (6.62)
\end{aligned}$$

We also note that

$$\|\phi_\sigma\| \le C\left(\|A^{1/2}(\phi_\sigma + \alpha\phi_p I)\| + \|\phi_p\|\right). \qquad (6.63)$$

Finally, combining (6.53), (6.62) and (6.63), we obtain

$$\begin{aligned}
&\|A^{1/2}(\phi_\sigma + \alpha\phi_p I)(t)\|^2 + \|\phi_\sigma(t)\|_{\mathrm{div}}^2 + \|\phi_u(t)\|^2 + \|\phi_\gamma(t)\|^2 + \|K^{-1/2}\phi_z(t)\|^2 + \|\phi_p(t)\|^2 \\
&\quad + \int_0^t \left(\|\phi_\sigma\|_{\mathrm{div}}^2 + \|\phi_u\|^2 + \|\phi_\gamma\|^2 + \|K^{-1/2}\phi_z\|^2 + \|\operatorname{div}\phi_z\|^2 + \|\phi_p\|^2\right) \\
&\le C\Big(h^2 \int_0^t \left(\|\partial_t\sigma\|_1^2 + \|\partial_t p\|_1^2 + \|\partial_t\gamma\|_1^2 + \|\partial_t z\|_1^2 + \|\sigma\|_1^2 + \|p\|_1^2 + \|\gamma\|_1^2 + \|z\|_1^2\right) ds \\
&\quad\quad + h^2\left(\|\sigma(t)\|_1^2 + \|p(t)\|_1^2 + \|\gamma(t)\|_1^2 + \|z(t)\|_1^2 + \|\sigma(0)\|_1^2\right) \\
&\quad\quad + \|\phi_\sigma(0)\|^2 + \|\phi_p(0)\|^2 + \|\phi_\gamma(0)\|^2 + \|\phi_z(0)\|^2\Big). \qquad (6.64)
\end{aligned}$$

For the initial error, we recall that the discrete initial data is taken to be the elliptic projection of the continuous initial data, see (4.10). Then, similarly to (5.16), we have

$$\|\phi_\sigma(0)\| + \|\phi_p(0)\| + \|\phi_\gamma(0)\| + \|\phi_z(0)\| \le C(\|\psi_\sigma(0)\| + \|\psi_p(0)\| + \|\psi_\gamma(0)\| + \|\psi_z(0)\| + \|\psi_u(0)\|). \qquad (6.65)$$

Bounds (6.64)–(6.65), combined with the use of the triangle inequality and the approximation bounds (6.7)–(6.11), imply the assertion of the theorem. □

7. Fully-discrete MSMFE–MFMFE method

In this section we present the fully-discrete method based on the backward Euler time discretization and show how the algebraic system at each time step can be reduced to a positive definite cell-centered displacement–pressure system.

Let $0 = t_0 < t_1 < \cdots < t_N = T$ be a partition of the time interval $[0, T]$ with time steps $\Delta t_n = t_n - t_{n-1}$, $n = 1, \ldots, N$, $\Delta t = \max_{1\le n\le N} \Delta t_n$. Let $\varphi^n = \varphi(t_n)$ and $\partial_t^n \varphi = (\varphi^n - \varphi^{n-1})/\Delta t_n$. For a Banach space H on Ω with a norm $\|\cdot\|_H$, we introduce the discrete-in-time norms

$$\|\varphi\|_{l^2(0,T;H)} := \left(\sum_{n=1}^{N} \Delta t_n \|\varphi\|_H^2\right)^{\frac{1}{2}}, \quad \|\varphi\|_{l^\infty(0,T;H)} := \max_{0\le n\le N} \|\varphi\|_H.$$

The fully-discrete MSMFE–MFMFE method is: given compatible initial data $(\sigma_h^0, u_h^0, \gamma_h^0, z_h^0, p_h^0)$, find, for $n = 1, \ldots, N$, $(\sigma_h^n, u_h^n, \gamma_h^n, z_h^n, p_h^n) \in \mathbb{X}_h \times V_h \times \mathbb{Q}_h \times Z_h \times W_h$ such that

$$\left(A(\sigma_h^n + \alpha p_h^n I), \tau\right)_Q + \left(u_h^n, \operatorname{div} \tau\right) + \left(\gamma_h^n, \tau\right)_Q = 0, \qquad \forall \tau \in \mathbb{X}_h, \tag{7.1}$$

$$-\left(\operatorname{div} \sigma_h^n, v\right) = \left(f^n, v\right), \qquad \forall v \in V_h, \tag{7.2}$$

$$\left(\sigma_h^n, \xi\right)_Q = 0, \qquad \forall \xi \in \mathbb{Q}_h, \tag{7.3}$$

$$\left(K^{-1} z_h^n, \zeta\right)_Q - \left(p_h^n, \operatorname{div} \zeta\right) = 0 \qquad \forall \zeta \in Z_h, \tag{7.4}$$

$$\left(c_0 \partial_t^n p_h, w\right) + \alpha \left(\partial_t^n A(\sigma_h + \alpha p_h I), wI\right)_Q + \left(\operatorname{div} z_h^n, w\right) = \left(q^n, w\right), \qquad \forall w \in W_h. \tag{7.5}$$

Lemma 7.1. *The fully discrete method (7.1)–(7.5) has a unique solution.*

Proof. The assertion of the lemma follows from the solvability of the resolvent system (4.5)–(4.9) shown in the proof of Theorem 4.2. □

The following convergence theorem can be proved using the framework in the proof of Theorem 6.1, combined with standard tools for treating the discrete time derivatives.

Theorem 7.1. *If $A \in W^{1,\infty}_{\mathcal{T}_h}$, $K^{-1} \in W^{1,\infty}_{\mathcal{T}_h}$, and the solution of (2.8)–(2.12) is sufficiently smooth, then there exists a positive constant C independent of h and c_0, such that the solution of (7.1)–(7.5) satisfies*

$$\begin{aligned}
&\|\sigma - \sigma_h\|_{l^\infty(0,T;H(\operatorname{div};\Omega))} + \|u - u_h\|_{l^\infty(0,T;L^2(\Omega))} + \|\gamma - \gamma_h\|_{l^\infty(0,T;L^2(\Omega))} + \|z - z_h\|_{l^\infty(0,T;L^2(\Omega))} \\
&\quad + \|p - p_h\|_{l^\infty(0,T;L^2(\Omega))} + \|\sigma - \sigma_h\|_{l^2(0,T;H(\operatorname{div};\Omega))} + \|u - u_h\|_{l^2(0,T;L^2(\Omega))} \\
&\quad + \|\gamma - \gamma_h\|_{l^2(0,T;L^2(\Omega))} + \|z - z_h\|_{l^2(0,T;H(\operatorname{div};\Omega))} + \|p - p_h\|_{l^2(0,T;L^2(\Omega))} \\
&\le Ch\Big(\|\sigma\|_{H^1(0,T;H^1(\Omega))} + \|\operatorname{div} \sigma\|_{L^\infty(0,T;H^1(\Omega))} + \|\operatorname{div} \sigma\|_{L^2(0,T;H^1(\Omega))} \\
&\quad + \|u\|_{L^2(0,T;H^1(\Omega))} + \|u\|_{L^\infty(0,T;H^1(\Omega))} + \|\gamma\|_{H^1(0,T;H^1(\Omega))} \\
&\quad + \|z\|_{H^1(0,T;H^1(\Omega))} + \|\operatorname{div} z\|_{L^2(0,T;H^1(\Omega))} + \|p\|_{H^1(0,T;H^1(\Omega))}\Big) \\
&\quad + C\Delta t \left(\|\sigma\|_{H^2(0,T;L^2(\Omega))} + \|u\|_{H^2(0,T;L^2(\Omega))} + \|\gamma\|_{H^2(0,T;L^2(\Omega))} + \|p\|_{H^2(0,T;L^2(\Omega))}\right).
\end{aligned} \tag{7.6}$$

7.1. Reduction to a cell-centered displacement–pressure system

The vertex quadrature rule applied to the stress and velocity bilinear forms, $\left(A\sigma_h^n, \tau\right)_Q$ in (7.1) and $\left(K^{-1} z_h^n, \zeta\right)_Q$ in (7.4), respectively results in the corresponding matrices $A_{\sigma\sigma}$ and A_{zz} being block-diagonal with blocks associated with the mesh vertices. More precisely, consider any interior vertex $\mathbf{r}$ shared by k edges or faces $e_1, \ldots, e_k$ as shown in Fig. 1. Let $\zeta_1, \ldots, \zeta_k$ be the velocity degrees of freedom associated with the vertex and let $z_1, \ldots, z_k$ be the corresponding normal velocity values, see Fig. 1(a). For the sake of visualization, the normal velocities are drawn at a distance from the vertex. The vertex quadrature rule $(K^{-1}\cdot, \cdot)_Q$ localizes the interaction of basis functions around each vertex by decoupling them from the rest of the basis functions, so taking $\zeta_1, \ldots, \zeta_k$ in (7.4) results in a local $k \times k$ linear system. Therefore A_{zz} is block-diagonal with $k \times k$ blocks associated with mesh vertices. Similarly, $A_{\sigma\sigma}$ is block-diagonal with $d\,k \times d\,k$ blocks, see Fig. 1(b). Due to the positive definiteness of A and K and Lemma 3.1, the blocks of $A_{\sigma\sigma}$ and A_{zz} are symmetric and positive definite. Therefore the velocity and stress can be easily eliminated by solving small local linear systems. Moreover, the rotation can be further eliminated as follows. Let $A_{\sigma\gamma}$ be the matrix corresponding to $\left(\sigma_h^n, \xi\right)_Q$ in (7.3). The localization of the basis function interaction around

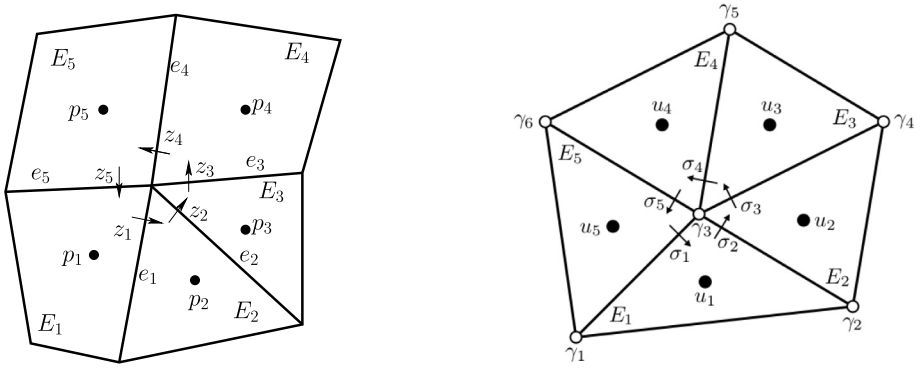

(a) Darcy degrees of freedom (b) Elasticity degrees of freedom

Fig. 1. Interactions of the degrees of freedom in the MSMFE–MFMFE method.

vertices due to the vertex quadrature rule implies that $A_{\sigma\gamma}$ is block-diagonal with $d(d-1)/2 \times dk$ blocks. After the stress elimination, the rotation matrix is $A_{\sigma\gamma}A_{\sigma\sigma}^{-1}A_{\sigma\gamma}^T$. Since $A_{\sigma\sigma}$ is block-diagonal with $dk \times dk$ blocks, then $A_{\sigma\gamma}A_{\sigma\sigma}^{-1}A_{\sigma\gamma}^T$ is block-diagonal with $d(d-1)/2 \times d(d-1)/2$ blocks. In fact, for $d = 2$ the matrix is diagonal. Each block couples the rotation degrees of freedom associated with the corresponding vertex. The blocks are symmetric and positive definite due to the inf–sup condition (4.2) and the positive definiteness of $A_{\sigma\sigma}^{-1}$. Therefore the rotation can be easily eliminated, resulting in a cell-centered displacement–pressure system. The above procedure can be expressed in matrix form as follows, where σ is the algebraic vector corresponding to σ_h^n, etc.:

$$
\begin{pmatrix} A_{\sigma\sigma} & A_{\sigma u}^T & A_{\sigma\gamma}^T & 0 & A_{\sigma p}^T \\ -A_{\sigma u} & 0 & 0 & 0 & 0 \\ -A_{\sigma\gamma} & 0 & 0 & 0 & 0 \\ 0 & 0 & 0 & A_{zz} & A_{zp}^T \\ A_{\sigma p} & 0 & 0 & -A_{zp} & A_{pp} \end{pmatrix} \begin{pmatrix} \sigma \\ u \\ \gamma \\ z \\ p \end{pmatrix}
$$

$$
\xrightarrow{\sigma = -A_{\sigma\sigma}^{-1}A_{\sigma u}^T u - A_{\sigma\sigma}^{-1}A_{\sigma\gamma}^T\gamma - A_{\sigma\sigma}^{-1}A_{\sigma p}^T p} \begin{pmatrix} A_{\sigma u}A_{\sigma\sigma}^{-1}A_{\sigma u}^T & A_{\sigma u}A_{\sigma\sigma}^{-1}A_{\sigma\gamma}^T & 0 & A_{\sigma u}A_{\sigma\sigma}^{-1}A_{\sigma p}^T \\ A_{\sigma\gamma}A_{\sigma\sigma}^{-1}A_{\sigma u}^T & A_{\sigma\gamma}A_{\sigma\sigma}^{-1}A_{\sigma\gamma}^T & 0 & A_{\sigma\gamma}A_{\sigma\sigma}^{-1}A_{\sigma p}^T \\ 0 & 0 & A_{zz} & A_{zp}^T \\ -A_{\sigma p}A_{\sigma\sigma}^{-1}A_{\sigma u}^T & -A_{\sigma p}A_{\sigma\sigma}^{-1}A_{\sigma\gamma}^T & -A_{zp} & A_{pp} - A_{\sigma p}A_{\sigma\sigma}^{-1}A_{\sigma p}^T \end{pmatrix} \begin{pmatrix} u \\ \gamma \\ z \\ p \end{pmatrix}
$$

$$
\xrightarrow{z = -A_{zz}^{-1}A_{zp}^T p} \begin{pmatrix} A_{u\sigma u} & A_{u\sigma\gamma} & A_{u\sigma p} \\ A_{u\sigma\gamma}^T & A_{\gamma\sigma\gamma} & A_{\gamma\sigma p} \\ -A_{u\sigma p}^T & -A_{\gamma\sigma p}^T & A_{p\sigma zp} \end{pmatrix} \begin{pmatrix} u \\ \gamma \\ p \end{pmatrix}
$$

$$
\xrightarrow{\gamma = -A_{\gamma\sigma\gamma}^{-1}A_{\gamma\sigma p}p - A_{\gamma\sigma\gamma}^{-1}A_{u\sigma\gamma}^T u} \begin{pmatrix} A_{u\sigma u} - A_{u\sigma\gamma}A_{\gamma\sigma\gamma}^{-1}A_{u\sigma\gamma}^T & A_{u\sigma p} - A_{u\sigma\gamma}A_{\gamma\sigma\gamma}^{-1}A_{\gamma\sigma p} \\ -A_{u\sigma p}^T + A_{\gamma\sigma p}^T A_{\gamma\sigma\gamma}^{-1}A_{u\sigma\gamma}^T & A_{p\sigma zp} + A_{\gamma\sigma p}^T A_{\gamma\sigma\gamma}^{-1}A_{\gamma\sigma p} \end{pmatrix} \begin{pmatrix} u \\ p \end{pmatrix}, \tag{7.7}
$$

where

$$
\begin{aligned}
A_{u\sigma u} &:= A_{\sigma u}A_{\sigma\sigma}^{-1}A_{\sigma u}^T, & A_{u\sigma\gamma} &:= A_{\sigma u}A_{\sigma\sigma}^{-1}A_{\sigma\gamma}^T, \\
A_{\gamma\sigma\gamma} &:= A_{\sigma\gamma}A_{\sigma\sigma}^{-1}A_{\sigma\gamma}^T, & A_{u\sigma p} &:= A_{\sigma u}A_{\sigma\sigma}^{-1}A_{\sigma p}^T, \\
A_{\gamma\sigma p} &:= A_{\sigma\gamma}A_{\sigma\sigma}^{-1}A_{\sigma p}^T, & A_{p\sigma zp} &:= A_{pp} - A_{\sigma p}A_{\sigma\sigma}^{-1}A_{\sigma p}^T + A_{zp}A_{zz}^{-1}A_{zp}^T.
\end{aligned}
$$

Remark 7.1. The expression $z = -A_{zz}^{-1}A_{zp}^T p$ above means that the normal velocity at each vertex is explicitly expressed in terms of the pressures at the centers of the elements that share that vertex, see also Fig. 1(a). Similarly, $\sigma = -A_{\sigma\sigma}^{-1}A_{\sigma u}^T u - A_{\sigma\sigma}^{-1}A_{\sigma\gamma}^T\gamma - A_{\sigma\sigma}^{-1}A_{\sigma p}^T p$ means that the normal stress at each vertex is expressed in terms of the displacements, rotations, and pressures at the centers of the elements that share the vertex. These expressions

motivate the terms multipoint flux and multipoint stress. They are used to recover the velocity and the stress after solving for the pressure and the displacement.

Proposition 7.1. *The cell-centered displacement–pressure matrix obtained in (7.7) is block-skew-symmetric and positive definite.*

Proof. Let us denote the four blocks of the matrix in (7.7) by A_{ij}, $i, j = 1, 2$. The block-skew-symmetric property follows from

$$-A_{12}^T = -(A_{u\sigma p} - A_{u\sigma\gamma}A_{\gamma\sigma\gamma}^{-1}A_{\gamma\sigma p})^T = -A_{u\sigma p}^T + A_{\gamma\sigma p}^T A_{\gamma\sigma\gamma}^{-1}A_{u\sigma\gamma}^T = A_{21},$$

using that $A_{\gamma\sigma\gamma}$ is symmetric. Therefore, for any $\begin{pmatrix} v^T & w^T \end{pmatrix} \neq 0$, we have

$$\begin{pmatrix} v^T & w^T \end{pmatrix} \begin{pmatrix} A_{11} & A_{12} \\ A_{21} & A_{22} \end{pmatrix} \begin{pmatrix} v \\ w \end{pmatrix} = v^T A_{11} v + w^T A_{22} w,$$

so we need to show that the diagonal blocks are positive definite. For A_{11} we have

$$A_{11} = A_{u\sigma u} - A_{u\sigma\gamma}A_{\gamma\sigma\gamma}^{-1}A_{u\sigma\gamma}^T = A_{\sigma u}A_{\sigma\sigma}^{-1}A_{\sigma u}^T - A_{\sigma u}A_{\sigma\sigma}^{-1}A_{\sigma\gamma}^T(A_{\sigma\gamma}A_{\sigma\sigma}^{-1}A_{\sigma\gamma}^T)^{-1}A_{\sigma\gamma}A_{\sigma\sigma}^{-1}A_{\sigma u}^T,$$

which is a Schur complement of the displacement–rotation matrix

$$\begin{pmatrix} A_{\sigma u}A_{\sigma\sigma}^{-1}A_{\sigma u}^T & A_{\sigma u}A_{\sigma\sigma}^{-1}A_{\sigma\gamma}^T \\ A_{\sigma\gamma}A_{\sigma\sigma}^{-1}A_{\sigma u}^T & A_{\sigma\gamma}A_{\sigma\sigma}^{-1}A_{\sigma\gamma}^T \end{pmatrix}.$$

The latter is symmetric and positive definite, since for any $\begin{pmatrix} v^T & \xi^T \end{pmatrix} \neq 0$,

$$\begin{pmatrix} v^T & \xi^T \end{pmatrix} \begin{pmatrix} A_{\sigma u}A_{\sigma\sigma}^{-1}A_{\sigma u}^T & A_{\sigma u}A_{\sigma\sigma}^{-1}A_{\sigma\gamma}^T \\ A_{\sigma\gamma}A_{\sigma\sigma}^{-1}A_{\sigma u}^T & A_{\sigma\gamma}A_{\sigma\sigma}^{-1}A_{\sigma\gamma}^T \end{pmatrix} \begin{pmatrix} v \\ \xi \end{pmatrix} = (A_{\sigma u}^T v + A_{\sigma\gamma}^T \xi)^T A_{\sigma\sigma}^{-1}(A_{\sigma u}^T v + A_{\sigma\gamma}^T \xi) > 0,$$

due to the positive definiteness of $A_{\sigma\sigma}$ and the elasticity inf–sup condition (4.2). Then A_{11} is also symmetric and positive definite, using [19, Theorem 7.7.6]. For A_{22} we have

$$A_{22} = A_{pp} - A_{\sigma p}A_{\sigma\sigma}^{-1}A_{\sigma p}^T + A_{zp}A_{zz}^{-1}A_{zp}^T + A_{\gamma\sigma p}^T A_{\gamma\sigma\gamma}^{-1}A_{\gamma\sigma p}.$$

The matrix $A_{pp} - A_{\sigma p}A_{\sigma\sigma}^{-1}A_{\sigma p}^T$ is positive semidefinite, using [19, Theorem 7.7.6], since it is a Schur complement of the matrix

$$A^{\sigma p} := \begin{pmatrix} A_{\sigma\sigma} & A_{\sigma p}^T \\ A_{\sigma p} & A_{pp} \end{pmatrix},$$

which is positive semidefinite, since $(\tau^T \; w^T)\, A^{\sigma p}\, (\tau \;\; w)^T = \|A^{1/2}(\tau_h + \alpha w_h I)\|_Q^2$. The middle matrix $A_{zp}A_{zz}^{-1}A_{zp}^T$ is positive definite, using that A_{zz} is positive definite and the Darcy inf–sup condition (4.1). Finally, the matrix $A_{\gamma\sigma p}^T A_{\gamma\sigma\gamma}^{-1}A_{\gamma\sigma p}$ is positive semidefinite, since $A_{\gamma\sigma\gamma}$ is positive definite. Combined, the three properties imply that A_{22} is symmetric and positive definite. □

Remark 7.2. The positive-definiteness of the matrix in (7.7) established in Proposition 7.1 allows for an efficient Krylov space iterative solver like GMRES to be used for the solution of the reduced displacement–pressure system. Moreover, since the diagonal blocks are symmetric and positive definite, the block-diagonal part of the matrix provides an efficient preconditioner.

8. Numerical results

The proposed fully discrete MSMFE–MFMFE method has been implemented on simplicial grids using the FEniCS Project [30] and on quadrilaterals using the deal.II finite element library [4]. In this section we provide several numerical tests verifying the theoretical convergence rates and illustrating the behavior of the method. We also present an example showing the locking-free property of the method in the case of a small storativity coefficient.

Table 1
Parameters for Examples 1.

Parameter	Symbol	Values
Lame coefficient	μ	100.0
Lame coefficient	λ	100.0
Mass storativity	c_0	1.0
Biot–Willis constant	α	1.0
Total time	T	10^{-3}
Time step	Δt	10^{-4}

8.1. Example 1

We first verify the convergence of the method on simplicial grids in three dimensions. We use the unit cube as a computational domain and choose the analytical solution for pressure and displacement as follows:

$$p = \cos(t)(x + y + z + 1.5), \quad u = \sin(t)\begin{pmatrix} -0.1(e^x - 1)\sin(\pi x)\sin(\pi y) \\ -(e^x - 1)(y - \cos(\frac{\pi}{12})(y - 0.5) + \sin(\frac{\pi}{12})(z - 0.5) - 0.5) \\ -(e^x - 1)(z - \sin(\frac{\pi}{12})(y - 0.5) - \cos(\frac{\pi}{12})(z - 0.5) - 0.5) \end{pmatrix}.$$

The permeability tensor is of the form

$$K = \begin{pmatrix} x^2 + y^2 + 1 & 0 & 0 \\ 0 & z^2 + 1 & \sin(xy) \\ 0 & \sin(xy) & x^2y^2 + 1 \end{pmatrix},$$

and the rest of the parameters are presented in Table 1.

Using the analytical solution provided above and Eqs. (2.3)–(2.4), we obtain the rest of variables and the right-hand side functions. Dirichlet boundary conditions for the pressure and the displacement are specified on the entire boundary of the domain.

In Table 2 we present the relative errors and spatial convergence rates on a sequence of mesh refinements. We take a sufficiently small time step $\Delta t = 10^{-4}$ to ensure that the time discretization error does not dominate. We observe at least first order of convergence in all norms, as predicted by the theory. The error $\|\gamma - \gamma_h\|$ exhibits convergence of order higher than one, which can be attributed to the linear polynomial approximation. The numerical solution on the finest level at the final time is shown in Fig. 2.

8.2. Example 2

In the second test case we study the convergence of the method on h^2-parallelogram grids. We consider the analytical solution

$$p = \exp(t)(\sin(\pi x)\cos(\pi y) + 10), \quad u = \exp(t)\begin{pmatrix} x^3y^4 + x^2 + \sin((1 - x)(1 - y))\cos(1 - y) \\ (1 - x)^4(1 - y)^3 + (1 - y)^2 + \cos(xy)\sin(x) \end{pmatrix},$$

and the permeability tensor

$$K = \begin{pmatrix} (x + 1)^2 + y^2 & \sin(xy) \\ \sin(xy) & (x + 1)^2 \end{pmatrix}.$$

In this example as elasticity parameters we use the Poisson ratio ν and the Young's modulus E. We set $\nu = 0.2$ and take E to vary over the domain, $E = \sin(5\pi x)\sin(5\pi y) + 5$. The Lamé parameters are then computed using the well known relations

$$\lambda = \frac{E\nu}{(1 + \nu)(1 - 2\nu)}, \quad \mu = \frac{E}{2(1 + \nu)}.$$

In this test case we also illustrate the behavior of the method for small mass storativity and set $c_0 = 10^{-5}$. The Biot–Willis constant α and the time discretization parameters are the same as in Table 1.

Table 2
Example 1, numerical errors and convergence rates.

h	$\|\sigma - \sigma_h\|_{L^2(0,T;L^2(\Omega))}$		$\|\mathrm{div}\,(\sigma - \sigma_h)\|_{L^2(0,T;L^2(\Omega))}$		$\|u - u_h\|_{L^2(0,T;L^2(\Omega))}$	
	Error	Rate	Error	Rate	Error	Rate
1/4	1.55E−02	–	2.29E−01	–	8.43E−01	–
1/8	4.97E−03	1.6	1.14E−01	1.0	2.30E−01	1.0
1/16	2.16E−03	1.2	5.65E−02	1.0	8.85E−02	1.0
1/32	1.03E−03	1.1	2.82E−02	1.0	4.11E−02	1.0
h	$\|\gamma - \gamma_h\|_{L^2(0,T;L^2(\Omega))}$		$\|z - z_h\|_{L^2(0,T;L^2(\Omega))}$		$\|\mathrm{div}\,(z - z_h)\|_{L^2(0,T;L^2(\Omega))}$	
	Error	Rate	Error	Rate	Error	Rate
1/4	7.65E−01	–	4.34E−04	–	5.85E−02	–
1/8	2.32E−01	1.7	2.26E−04	0.9	2.31E−02	1.3
1/16	7.04E−02	1.7	1.14E−04	1.0	1.05E−02	1.1
1/32	2.13E−02	1.7	5.68E−05	1.0	5.00E−03	1.1
h	$\|p - p_h\|_{L^2(0,T;L^2(\Omega))}$		$\|\sigma - \sigma_h\|_{L^\infty(0,T;L^2(\Omega))}$		$\|u - u_h\|_{L^\infty(0,T;L^2(\Omega))}$	
	Error	Rate	Error	Rate	Error	Rate
1/4	2.58E−01	–	2.29E−01	–	2.55E+00	–
1/8	1.26E−01	1.0	1.14E−01	1.0	7.12E−01	1.8
1/16	6.18E−02	1.0	5.67E−02	1.0	2.91E−01	1.3
1/32	3.09E−02	1.0	2.82E−02	1.0	1.38E−01	1.1
h	$\|\gamma - \gamma_h\|_{L^\infty(0,T;L^2(\Omega))}$		$\|z - z_h\|_{L^\infty(0,T;L^2(\Omega))}$		$\|p - p_h\|_{L^\infty(0,T;L^2(\Omega))}$	
	Error	Rate	Error	Rate	Error	Rate
1/4	2.35E+00	–	4.78E−04	–	2.58E−01	–
1/8	7.06E−01	1.7	2.57E−04	0.9	1.26E−01	1.0
1/16	2.12E−01	1.7	1.33E−04	0.9	6.21E−02	1.0
1/32	6.37E−02	1.7	6.69E−05	1.0	3.09E−02	1.0

The computational domain for this case is obtained as follows. We start with the unit square and partition it into a 4×4 square mesh with $h = \frac{1}{4}$. We then move the mesh points using the map

$$x = \hat{x} + 0.03\cos(3\pi\hat{x})\cos(3\pi\hat{y}), \quad y = \hat{y} - 0.04\cos(3\pi\hat{x})\cos(3\pi\hat{y}),$$

which gives a deformed computational domain with a 4×4 quadrilateral grid, see Fig. 3. A sequence of mesh refinements is obtained by a uniform refinement of the elements of the coarse grid. The resulting sequence of meshes satisfies the h^2-parallelogram property (6.1).

As in the previous test case, we observe at least first order convergence for all variables in their respective norms, see Table 3. The computed solution with $h = \frac{1}{32}$ at the final time is shown in Fig. 3. This example not only confirms the theoretical convergence rates on h^2-parallelogram grids, but also illustrates that the method can handle well variable elasticity parameters and small mass storativity.

8.3. Example 3

We next focus on studying the locking-free properties of the MSMFE–MFMFE method when applied to the solution of a two-dimensional footing problem [17,37]. A load of given intensity σ_0 is applied along a strip along the top of a rectangular block of porous, saturated, and deformable soil. The lateral sides and the bottom of the block are fixed. The entire boundary is free to drain. The computational domain is $\Omega = [-50, 50] \times [0, 75]$. We label the middle section of the top boundary, $x \in [-50/3, 50/3]$, $y = 75$, by Γ_1, the rest of the top side by Γ_2, and all other boundaries by Γ_3. The boundary conditions are as follows:

$$\begin{aligned}
&\sigma\, n = (0, -\sigma_0)^T, && \text{on } \Gamma_1,\\
&\sigma\, n = (0, 0)^T, && \text{on } \Gamma_2,\\
&u = (0, 0)^T, && \text{on } \Gamma_3,\\
&p = 0, && \text{on } \partial\Omega.
\end{aligned}$$

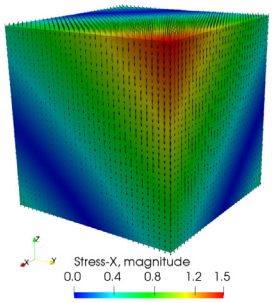

(a) Stress, x-component

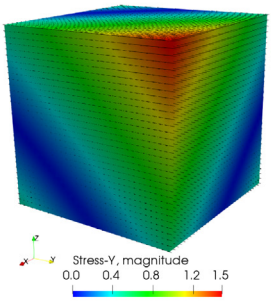

(b) Stress, y-component

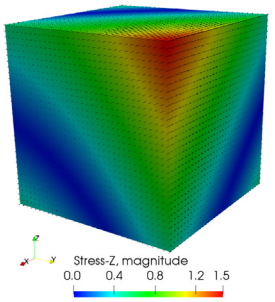

(c) Stress, z-component

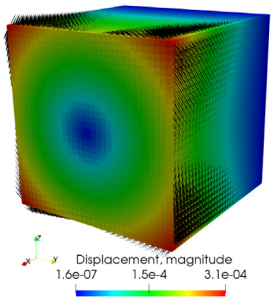

(d) Displacement

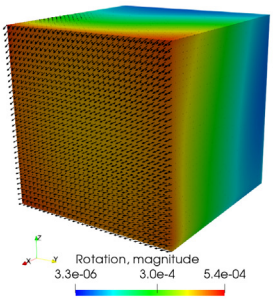

(e) Rotation

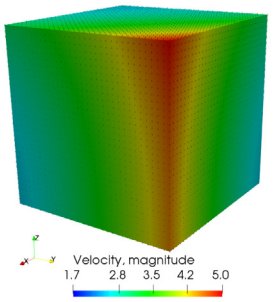

(f) Darcy velocity

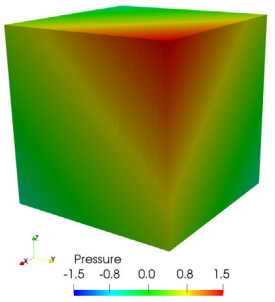

(g) Darcy pressure

Fig. 2. Example 1, computed solution with $h = \frac{1}{32}$ at the final time.

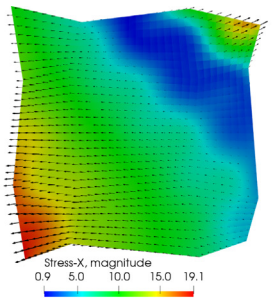

(a) Stress, x-component

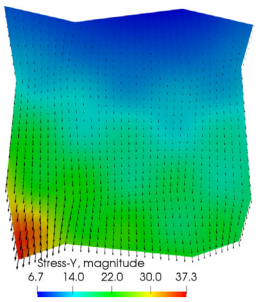

(b) Stress, y-component

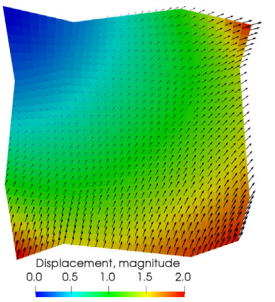

(c) Displacement

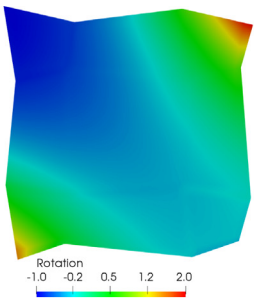

(d) Rotation

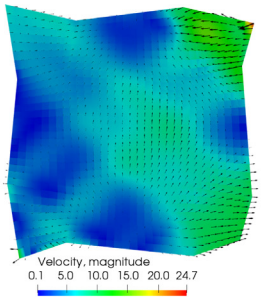

(e) Darcy velocity

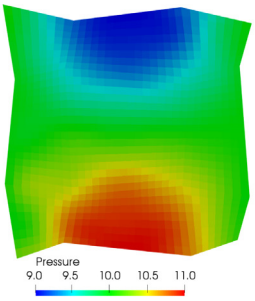

(f) Darcy pressure

Fig. 3. Example 2, computed solution with $h = \frac{1}{32}$ at the final time.

Table 3
Example 2, numerical errors and convergence rates.

h	$\|\sigma - \sigma_h\|_{L^2(0,T;L^2(\Omega))}$		$\|\mathrm{div}\,(\sigma - \sigma_h)\|_{L^2(0,T;L^2(\Omega))}$		$\|u - u_h\|_{L^2(0,T;L^2(\Omega))}$	
	Error	Rate	Error	Rate	Error	Rate
1/8	9.65E−02	–	1.30E−01	–	8.02E−02	–
1/16	4.97E−02	1.0	6.46E−02	1.0	3.97E−02	1.0
1/32	2.52E−02	1.0	3.23E−02	1.0	1.98E−02	1.0
1/64	1.27E−02	1.0	1.61E−02	1.0	9.87E−03	1.0
1/128	6.35E−03	1.0	8.07E−03	1.0	4.93E−03	1.0
h	$\|\gamma - \gamma_h\|_{L^2(0,T;L^2(\Omega))}$		$\|z - z_h\|_{L^2(0,T;L^2(\Omega))}$		$\|\mathrm{div}\,(z - z_h)\|_{L^2(0,T;L^2(\Omega))}$	
	Error	Rate	Error	Rate	Error	Rate
1/8	2.03E−01	–	1.44E−01	–	2.88E−01	–
1/16	7.51E−02	1.4	7.05E−02	1.0	1.75E−01	0.7
1/32	2.77E−02	1.4	3.47E−02	1.0	8.18E−02	1.1
1/64	1.02E−02	1.5	1.72E−02	1.0	3.35E−02	1.3
1/128	3.70E−03	1.5	8.60E−03	1.0	1.39E−02	1.3
h	$\|p - p_h\|_{L^2(0,T;L^2(\Omega))}$		$\|\sigma - \sigma_h\|_{L^\infty(0,T;L^2(\Omega))}$		$\|u - u_h\|_{L^\infty(0,T;L^2(\Omega))}$	
	Error	Rate	Error	Rate	Error	Rate
1/8	8.97E−03	–	9.65E−02	–	8.02E−02	–
1/16	4.49E−03	1.0	4.97E−02	1.0	3.97E−02	1.0
1/32	2.24E−03	1.0	2.52E−02	1.0	1.98E−02	1.0
1/64	1.12E−03	1.0	1.27E−02	1.0	9.87E−03	1.0
1/128	5.61E−04	1.0	6.35E−03	1.0	4.93E−03	1.0
h	$\|\gamma - \gamma_h\|_{L^\infty(0,T;L^2(\Omega))}$		$\|z - z_h\|_{L^\infty(0,T;L^2(\Omega))}$		$\|p - p_h\|_{L^\infty(0,T;L^2(\Omega))}$	
	Error	Rate	Error	Rate	Error	Rate
1/8	2.03E−01	–	1.60E−01	–	9.03E−03	–
1/16	7.51E−02	1.4	8.07E−02	1.0	4.50E−03	1.0
1/32	2.77E−02	1.4	3.69E−02	1.1	2.24E−03	1.0
1/64	1.02E−02	1.5	1.75E−02	1.1	1.12E−03	1.0
1/128	3.70E−03	1.5	8.64E−03	1.0	5.61E−04	1.0

The model parameters are: Young's modulus $E = 3 \cdot 10^4$ (N/m^2), permeability $K = 10^{-4}$ (m^2/Pa), load intensity $\sigma_0 = 10^4$ (N/m^2) and mass storativity $c_0 = 0.001$. We test the behavior of the method in the incompressibility limit by setting Poisson ratio $\nu = 0.4995$. The initial pressure and displacement are set to zero. We discretize the domain into 62025 unstructured simplices and solve the problem for total time of $T = 50$s using time step of size $\Delta t = 1$s.

It is observed in [17,37] that for this value of the Poisson ratio, inf–sup unstable discretizations may result in spurious pressure modes and/or locking in the computed displacement. In Fig. 4 we show the solution obtained by MSMFE–MFMFE method at the final time. For visualization purpose, the solution is plotted on the deformed domain. Neither spurious oscillations in the pressure, nor locking effects in the displacement are present, illustrating that the proposed method inherits the locking-free properties of the classical mixed method it is derived from. We further note the smooth stress approximation and the accurate resolution of the pressure and velocity boundary layers, as well as the rotation singularities.

8.4. Example 4

In the last example we further illustrate the locking-free properties of the MSMFE–MFMFE method in a different parameter regime. It is shown in [41] that, with continuous finite elements for the elasticity part of the system, locking occurs when the storativity and permeability coefficients are very small. In this regime, the locking is exhibited as spurious pressure oscillations at early times. A typical model problem that illustrates such behavior is the cantilever bracket problem [29]. The computational domain is the unit square. We impose a no-flow boundary condition along all sides. The deformation is fixed along the left edge, and a downward traction is applied along the

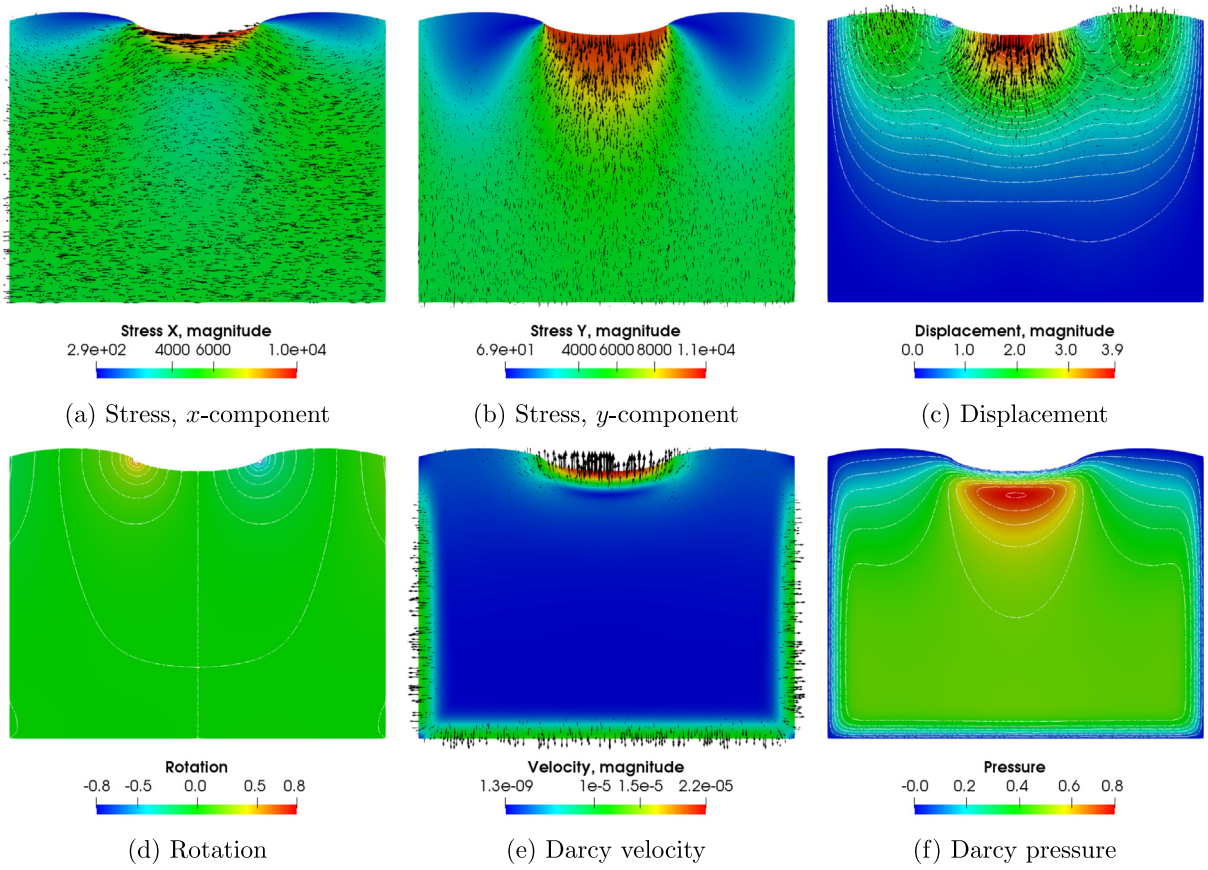

(a) Stress, x-component (b) Stress, y-component (c) Displacement

(d) Rotation (e) Darcy velocity (f) Darcy pressure

Fig. 4. Example 3, computed solution at the final time on the deformed domain.

top. The bottom and right sides are traction-free. More precisely, with the sides of the domain labeled as $\Gamma_1, \ldots, \Gamma_4$, starting from the bottom side and going counterclockwise, we impose

$$
\begin{aligned}
&z \cdot n = 0, && \text{on } \partial\Omega = \Gamma_1 \cup \Gamma_2 \cup \Gamma_3 \cup \Gamma_4,\\
&\sigma\, n = (0,-1)^T, && \text{on } \Gamma_3,\\
&\sigma\, n = (0,0)^T, && \text{on } \Gamma_1 \cup \Gamma_2,\\
&u = (0,0)^T, && \text{on } \Gamma_4.
\end{aligned}
$$

We use the same physical parameters as in [41], as they typically induce locking:

$$E = 10^5, \quad \nu = 0.4, \quad \alpha = 0.93, \quad c_0 = 0, \quad K = 10^{-7}.$$

The time step is $\Delta t = 0.001$ and the total simulation time is $T = 1$.

Fig. 5(a) shows that the MSMFE–MFMFE method yields a smooth pressure field, in contrast to the non-physical checkerboard pattern that one obtains with continuous elasticity elements at the early time steps, see [41]. In addition, Fig. 5(b) shows the pressure solution along different x-lines at time $t = 0.005$. It illustrates the lack of oscillations and shows that our solution agrees with the one obtained by DG-mixed or stabilized CG-mixed discretizations [29,41]. We remark that our method requires solving a much smaller algebraic system than these two methods, which furthermore is positive definite and more efficient to solve.

Declaration of competing interest

The authors declare that they have no known competing financial interests or personal relationships that could have appeared to influence the work reported in this paper.

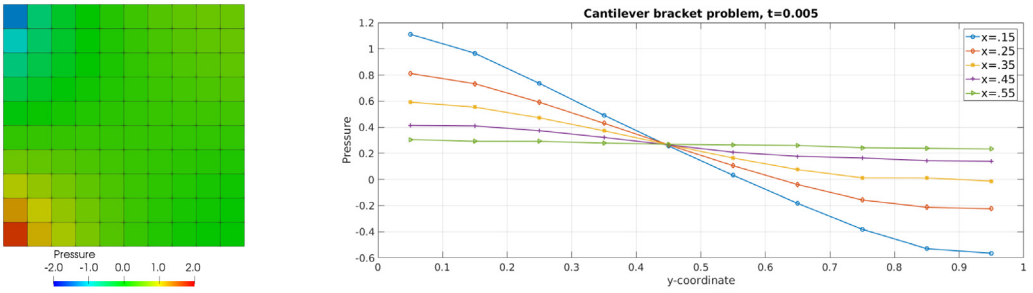

(a) Pressure field, $t = 0.001$. (b) Pressure along different $x-$lines, $t = 0.005$.

Fig. 5. Example 3, computed pressure solutions.

References

[1] I. Aavatsmark, T. Barkve, O. Bøe, T. Mannseth, Discretization on unstructured grids for inhomogeneous, anisotropic media. I. Derivation of the methods, SIAM J. Sci. Comput. 19 (5) (1998) 1700–1716.

[2] I. Ambartsumyan, E. Khattatov, J.M. Nordbotten, I. Yotov, A multipoint stress mixed finite element method for elasticity on quadrilateral grids, submitted for publication. arXiv:1811.01928 [math.NA].

[3] I. Ambartsumyan, E. Khattatov, J.M. Nordbotten, I. Yotov, A multipoint stress mixed finite element method for elasticity on simplicial grids, SIAM J. Numer. Anal. 58 (1) (2020) 630–656.

[4] D. Arndt, W. Bangerth, D. Davydov, T. Heister, L. Heltai, M. Kronbichler, M. Maier, J.-P. Pelteret, B. Turcksin, D. Wells, The `deal.II` library, version 8.5, J. Numer. Math. 25 (3) (2017) 137–146.

[5] D.N. Arnold, G. Awanou, W. Qiu, Mixed finite elements for elasticity on quadrilateral meshes, Adv. Comput. Math. 41 (3) (2015) 553–572.

[6] D.N. Arnold, D. Boffi, R.S. Falk, Quadrilateral $H(\mathrm{div})$ finite elements, SIAM J. Numer. Anal. 42 (6) (2005) 2429–2451.

[7] D.N. Arnold, R.S. Falk, R. Winther, Mixed finite element methods for linear elasticity with weakly imposed symmetry, Math. Comp. 76 (260) (2007) 1699–1723.

[8] M.A. Biot, General theory of three-dimensional consolidation, J. Appl. Phys. 12 (2) (1941) 155–164.

[9] D. Boffi, F. Brezzi, L.F. Demkowicz, R.G. Durán, R.S. Falk, M. Fortin, Mixed Finite Elements, Compatibility Conditions, and Applications, in: Lecture Notes in Mathematics, vol. 1939, Springer-Verlag, Berlin; Fondazione C.I.M.E., Florence, 2008, p. x+235, Lectures given at the C.I.M.E. Summer School held in Cetraro, June 26–July 1, 2006, Edited by Boffi and Lucia Gastaldi.

[10] D. Boffi, F. Brezzi, M. Fortin, Reduced symmetry elements in linear elasticity, Commun. Pure Appl. Anal. 8 (1) (2009) 95–121.

[11] D. Boffi, F. Brezzi, M. Fortin, Mixed Finite Element Methods and Applications, in: Springer Series in Computational Mathematics, vol. 44, Springer, Heidelberg, 2013, p. xiv+685.

[12] F. Brezzi, J. Douglas Jr., L.D. Marini, Two families of mixed finite elements for second order elliptic problems, Numer. Math. 47 (2) (1985) 217–235.

[13] F. Brezzi, M. Fortin, L.D. Marini, Error analysis of piecewise constant pressure approximations of Darcy's law, Comput. Methods Appl. Mech. Engrg. 195 (2006) 1547–1559.

[14] P.G. Ciarlet, The Finite Element Method for Elliptic Problems, in: Studies in Mathematics and its Applications, vol. 4, North-Holland Publishing Co., Amsterdam-New York-Oxford, 1978, p. xix+530.

[15] M.G. Edwards, C.F. Rogers, Finite volume discretization with imposed flux continuity for the general tensor pressure equation, Comput. Geosci. 2 (4) (1998) 259–290 (1999).

[16] M. Farhloul, M. Fortin, Dual hybrid methods for the elasticity and the Stokes problems: a unified approach, Numer. Math. 76 (4) (1997) 419–440.

[17] F.J. Gaspar, F.J. Lisbona, C.W. Oosterlee, A stabilized difference scheme for deformable porous media and its numerical resolution by multigrid methods, Comput. Vis. Sci. 11 (2) (2008) 67–76.

[18] F.J. Gaspar, F.J. Lisbona, P.N. Vabishchevich, A finite difference analysis of Biot's consolidation model, Appl. Numer. Math. 44 (4) (2003) 487–506.

[19] R.A. Horn, C.R. Johnson, Matrix Analysis, second ed., Cambridge University Press, Cambridge, 2013, p. xviii+643.

[20] X. Hu, C. Rodrigo, F.J. Gaspar, L.T. Zikatanov, A nonconforming finite element method for the Biot's consolidation model in poroelasticity, J. Comput. Appl. Math. 310 (2017) 143–154.

[21] R. Ingram, M.F. Wheeler, I. Yotov, A multipoint flux mixed finite element method on hexahedra, SIAM J. Numer. Anal. 48 (4) (2010) 1281–1312.

[22] E. Keilegavlen, J.M. Nordbotten, Finite volume methods for elasticity with weak symmetry, Internat. J. Numer. Methods Engrg. 112 (8) (2017) 939–962.

[23] R.A. Klausen, R. Winther, Robust convergence of multi point flux approximation on rough grids, Numer. Math. 104 (3) (2006) 317–337.

[24] J. Korsawe, G. Starke, A least-squares mixed finite element method for Biot's consolidation problem in porous media, SIAM J. Numer. Anal. 43 (1) (2005) 318–339.

[25] J.J. Lee, Robust error analysis of coupled mixed methods for Biot's consolidation model, J. Sci. Comput. 69 (2) (2016) 610–632.
[26] J.J. Lee, Towards a unified analysis of mixed methods for elasticity with weakly symmetric stress, Adv. Comput. Math. 42 (2) (2016) 361–376.
[27] J.J. Lee, Robust three-field finite element methods for Biot's consolidation model in poroelasticity, BIT 58 (2) (2018) 347–372.
[28] J.J. Lee, K.-A. Mardal, R. Winther, Parameter-robust discretization and preconditioning of Biot's consolidation model, SIAM J. Sci. Comput. 39 (1) (2017) A1–A24.
[29] R. Liu, Discontinuous Galerkin Finite Element Solution for Poromechanics (Ph.D. thesis), The University of Texas at Austin, 2004.
[30] A. Logg, K.-A. Mardal, G.N. Wells, et al., Automated Solution of Differential Equations by the Finite Element Method, Springer, 2012.
[31] M.A. Murad, A.F.D. Loula, Improved accuracy in finite element analysis of Biot's consolidation problem, Comput. Methods Appl. Mech. Engrg. 95 (3) (1992) 359–382.
[32] J.-C. Nédélec, Mixed finite elements in $\mathbf{R}^3$, Numer. Math. 35 (3) (1980) 315–341.
[33] J.-C. Nédélec, A new family of mixed finite elements in $\mathbf{R}^3$, Numer. Math. 50 (1) (1986) 57–81.
[34] J.M. Nordbotten, Cell-centered finite volume discretizations for deformable porous media, Internat. J. Numer. Methods Engrg. 100 (6) (2014) 399–418.
[35] J.M. Nordbotten, Convergence of a cell-centered finite volume discretization for linear elasticity, SIAM J. Numer. Anal. 53 (6) (2015) 2605–2625.
[36] J.M. Nordbotten, Stable cell-centered finite volume discretization for Biot equations, SIAM J. Numer. Anal. 54 (2) (2016) 942–968.
[37] R. Oyarzúa, R. Ruiz-Baier, Locking-free finite element methods for poroelasticity, SIAM J. Numer. Anal. 54 (5) (2016) 2951–2973.
[38] P.J. Phillips, M.F. Wheeler, A coupling of mixed and continuous Galerkin finite element methods for poroelasticity. I. The continuous in time case, Comput. Geosci. 11 (2) (2007) 131–144.
[39] P.J. Phillips, M.F. Wheeler, A coupling of mixed and continuous Galerkin finite element methods for poroelasticity. II. the discrete-in-time case, Comput. Geosci. 11 (2) (2007) 145–158.
[40] P.J. Phillips, M.F. Wheeler, A coupling of mixed and discontinuous Galerkin finite-element methods for poroelasticity, Comput. Geosci. 12 (4) (2008) 417–435.
[41] P.J. Phillips, M.F. Wheeler, Overcoming the problem of locking in linear elasticity and poroelasticity: an heuristic approach, Computat. Geosci. 13 (1) (2009) 5.
[42] P.-A. Raviart, J.M. Thomas, A mixed finite element method for 2nd order elliptic problems, in: Mathematical Aspects of the Finite Element Method, in: Lecture Notes in Mathematics, vol. 606, Springer-Verlag, New York, 1977, pp. 292–315.
[43] J.E. Roberts, J.-M. Thomas, Mixed and hybrid methods, in: Handbook of Numerical Analysis, vol. II, in: Handb. Numer. Anal., II, North-Holland, Amsterdam, 1991, pp. 523–639.
[44] C. Rodrigo, F.J. Gaspar, X. Hu, L.T. Zikatanov, Stability and monotonicity for some discretizations of the Biot's consolidation model, Comput. Methods Appl. Mech. Engrg. 298 (2016) 183–204.
[45] C. Rodrigo, X. Hu, P. Ohm, J.H. Adler, F.J. Gaspar, L.T. Zikatanov, New stabilized discretizations for poroelasticity and the Stokes' equations, Comput. Methods Appl. Mech. Engrg. 341 (2018) 467–484.
[46] R.E. Showalter, Diffusion in poro-elastic media, J. Math. Anal. Appl. 251 (1) (2000) 310–340.
[47] R.E. Showalter, Nonlinear degenerate evolution equations in mixed formulation, SIAM J. Math. Anal. 42 (5) (2010) 2114–2131.
[48] R.E. Showalter, Monotone Operators in Banach Space and Nonlinear Partial Differential Equations, vol. 49, American Mathematical Soc., 2013.
[49] J. Wang, T. Mathew, Mixed finite element methods over quadrilaterals, in: I. Dimov, B. Sendov, P. Vassilevski (Eds.), Conference on Advances in Numerical Methods and Applications, World Scientific, River Edge, NJ, 1994, pp. 203–214.
[50] M.F. Wheeler, G. Xue, I. Yotov, A multipoint flux mixed finite element method on distorted quadrilaterals and hexahedra, Numer. Math. 121 (1) (2012) 165–204.
[51] M.F. Wheeler, G. Xue, I. Yotov, A multiscale mortar multipoint flux mixed finite element method, ESAIM Math. Model. Numer. Anal. 46 (4) (2012) 759–796.
[52] M.F. Wheeler, I. Yotov, A multipoint flux mixed finite element method, SIAM J. Numer. Anal. 44 (5) (2006) 2082–2106.
[53] S.-Y. Yi, A coupling of nonconforming and mixed finite element methods for Biot's consolidation model, Numer. Methods Partial Differential Equations 29 (5) (2013) 1749–1777.
[54] S.-Y. Yi, Convergence analysis of a new mixed finite element method for Biot's consolidation model, Numer. Methods Partial Differential Equations 30 (4) (2014) 1189–1210.
[55] S.-Y. Yi, A study of two modes of locking in poroelasticity, SIAM J. Numer. Anal. 55 (4) (2017) 1915–1936.